Journal of Structural Geology 175 (2023) 104954

Contents lists available at ScienceDirect

Journal of Structural Geology

journal homepage: www.elsevier.com/locate/jsg

# Natural fractures in ultra-deep reservoirs of China: A review

Lianbo Zeng [a,b,c,*], Yichen Song [b], Guoping Liu [c], Xiaolin Tan [b], Xiaotong Xu [b], Yingtao Yao [b], Zhe Mao [b]

[a] State Key Laboratory of Petroleum Resources and Prospecting, China University of Petroleum, Beijing, 102249, China
[b] College of Geosciences, China University of Petroleum, Beijing, 102249, China
[c] Institute of Energy, Peking University, Beijing, 100871, China

ARTICLE INFO

*Keywords:*
Natural fractures
Ultra-deep strata
Sandstone reservoirs
Carbonate reservoirs
Fracture effectiveness
Fault-related folds
Strike-slip faults

ABSTRACT

In recent years, China has made significant progress in exploring oil and gas in sandstone and carbonate rocks with burial depths of more than 6000 m in the Tarim, Sichuan, and Junggar Basins. These ultra-deep reservoirs have widely developed natural fractures that are important storage spaces and primary flow pathways influencing hydrocarbon enrichment and production. For ultra-deep tight sandstone, fractures caused by tectonic, diagenetic, tectonic-diagenetic, and overpressure processes are widespread. In the foreland thrust belt, which is divided into five fracture domains, fault-related folds affect fracture distribution in ultra-deep sandstones. For ultra-deep carbonate rocks, strike-slip faults control scale, structural style, and linkage evolution of fractures. Fractures formed over multiple periods. Many fractures in Cretaceous sandstones formed recently whereas some of those in carbonate rocks formed in the Paleozoic when strata were buried less than 5000 m. With the increase in burial depth, fracture porosity (and, probably) connectivity is reduced by mineral deposits. Fracture-forming processes include overpressure, present in situ burial and tectonic loading. Other variables modifying fractures include when fractures formed (timing), regional and local structural position, and scale and fluid flow leading to heterogeneity in whether fractures are mineral filled, open, or enhanced by dissolution. Our review provides insights into the origins, characteristics, evolution, and effectiveness of fractures in ultra-deep sandstone and carbonate rocks.

## Author statement

Lianbo Zeng: Conceptualization, Formal analysis, Writing-Reviewing and Editing.
Yichen Song: Writing-Original draft preparation, Methodology.
Guoping Liu: Writing-Reviewing and Editing.
Xiaolin Tan: Visualization, Investigation.
Xiaotong Xu: Visualization, Investigation.
Yingtao Yao: Software, Data curation.
Zhe Mao: Methodology, Software.

## 1. Introduction

Internationally, the definition of deep basins generally adopts the 4500 m standard set by the United States Geological Survey and some former Soviet scholars (Barker and Takach, 1992). In China rocks in sedimentary basins with burial depths of 4500–6000 m are defined as deep, and those with a burial depth greater than 6000 m are ultra-deep (Sun et al., 2013; Liu et al., 2021; Laubach et al., 2023). Core, image log observations, and production responses show that these deeply buried rocks contain a wide range of fracture types in considerable abundance and that in many cases such fractures are open and make effective fluid flow conduits. An extensive literature published in the past few years provides important insights into deep basin brittle structure that typically can only be inferred from outcrop analogs or indirect measures like well production response, but the size of the literature, the diversity of basins, subbasins, and structures, and the immense area of central and east Asia whence observations come, have impeded appreciation of these findings. Here we provide a summary and evaluation of this literature.

Fracture information is being collected and reported because deep and ultra-deep reservoirs are significant targets for oil and gas exploration and development. Recently breakthroughs in exploiting such reservoirs have been made in the Tarim, Sichuan, Junggar, Ordos, and

* Corresponding author. State Key Laboratory of Petroleum Resources and Prospecting, China University of Petroleum, Beijing, 102249, China.
*E-mail address:* lbzeng@sina.com (L. Zeng).

https://doi.org/10.1016/j.jsg.2023.104954
Received 24 October 2022; Received in revised form 11 September 2023; Accepted 13 September 2023
Available online 16 September 2023
0191-8141/

Bohai Bay Basins (Fig. 1) (Sun et al., 2013; Guo et al., 2018; Li et al., 2021b; Ma et al., 2022). Deep and ultra-deep reservoirs are concentrated in Mesozoic and Paleogene continental clastic rocks and Paleozoic marine carbonate rocks. Of these Mesozoic and Paleogene continental clastic reservoirs are mainly in the Tarim and Junggar Basins in western China, and the Paleozoic marine carbonate reservoirs are primarily within the Tarim, Sichuan, and Ordos Basins in central and west China (Zhao et al., 2011; Sun et al., 2013; He et al., 2016; Wang et al., 2019b). Furthermore, there are deep basement reservoirs in the Bohai Bay Basin of eastern China, including some in Proterozoic and Paleozoic marine carbonate and Archean metamorphic rocks (Zhao et al., 2013; Liu et al., 2020). Additionally, oil and gas explorations in volcanic, shale, and other reservoirs have gradually expanded into deep and ultra-deep fields, yielding essential discoveries in areas such as Sichuan and Junggar Basins (Zou et al., 2014; Guo, 2016; Ma et al., 2021; Peng et al., 2022).

These reservoirs are deep and in rocks undergoing active tectonic shortening and rapid burial or uplift (e.g., Ni, 1978; Rizza et al., 2019). In the current high-strain-rate regime, corroborated by velocity gradient tensor analysis of global positioning system (GPS) data, a rapid horizontal extension could promote the connection of porous and/or solution-enlarged fault rocks, fractures, and cavities (Bosworth et al., 2005; Ukar et al., 2020). Although some fractures in these ultradeep settings are old and have persisted for tens or hundreds of millions of years, data from wells in these reservoirs provide an exceptional view of deep fracture formation under the influence of active tectonics that differs markedly from, for example, deep reservoirs in the western United States, where the tectonic conditions that drove fracture formation have in most instances become quiescent in the last 20 to 50 Ma (e.g., Laubach et al., 2016).

Here we systematically review natural fractures in ultra-deep reservoirs in China based on recent and published work. Our focus is on ultra-deep tight sandstone and carbonate reservoirs. The datasets primarily come from geological observations of cores and thin sections, geophysical data such as seismic and image logs, and geochemical data such as isotopic and fluid inclusion measurements. We summarize the fracture types, characteristics, and distribution patterns with emphasis on fault-related folds in ultra-deep tight sandstone reservoirs and strike-slip faults in ultra-deep carbonate reservoirs. Finally, we discuss the time of fracture formation and the effectiveness of fractures (i.e., their capacity to maintain and enhance permeability), and the factors controlling dynamic evolution of ultra-deep reservoirs. This review provides references for a systematic understanding of natural fractures in ultra-deep reservoirs in China and facilitates hydrocarbon exploration and favorable reservoir evaluation in such reservoirs.

## 2. Deep basins and fractures in China

Ultra-deep oil and gas exploration in China mainly focuses on the Tarim, Sichuan, and Junggar Basins (Table 1). Ultra-deep oil and gas exploration in the Tarim Basin started in 2008, and hydrocarbon reserves discovered in ultra-deep reservoirs have accounted for more than 90% of China's total reserves and about 19% of global reserves since 2013 (Sun et al., 2013; Jia and Pang, 2015; Yang et al., 2021).

The ultra-deep reservoirs in the Tarim Basin comprise tight continental sandstones of the Upper Cretaceous Bashijiqike Formation distributed in the Kuqa Depression and marine carbonate rocks of the Middle-Lower Ordovician Yingshan Formation and Yijianfang Formation distributed (Yang et al., 2021). The ultra-deep reservoirs in the Sichuan Basin include Permian and Triassic marine carbonate rocks, and those in the central and southern Junggar Basin mainly include Jurassic and Cretaceous tight sandstones (Dai et al., 2021; Gan et al., 2022). For ultra-deep tight sandstone and carbonate rocks in China, the complex superposition of tectonism and diagenesis not only forms tight reservoirs

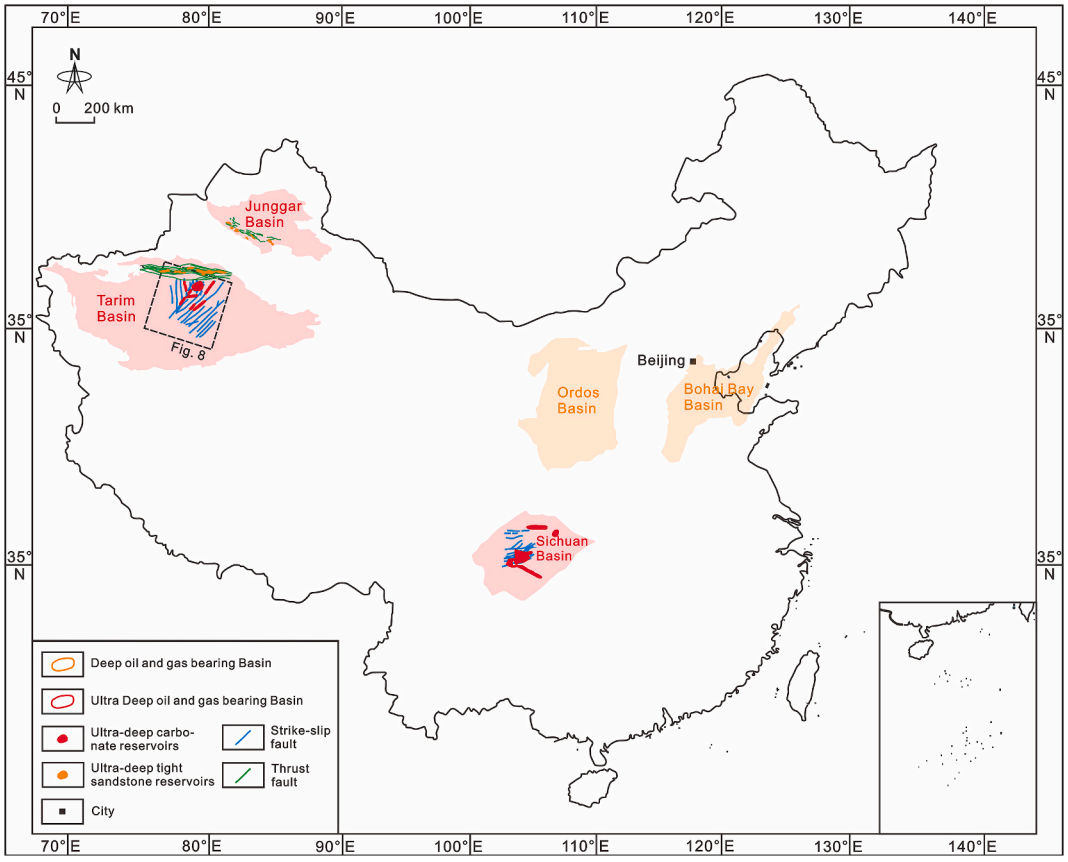


**Fig. 1.** Deep and ultra-deep oil and gas-bearing basins in China. The location of Fig. 8 is shown.

**Table 1**
The ultra-deep oil and gas reservoirs found in China.

| Oil and gas fields | Basins | Depth/m | Formations | Lithologies | References |
|---|---|---|---|---|---|
| Tahe | Tarim | 5400–8400 | Middle-Lower Ordovician Yingshan Formation and Yijianfang Formation | Grainstone; Micrite | He et al. (2016) |
| Shunbei | Tarim | > 7000 | Middle-Lower Ordovician Yingshan Formation and Yijianfang Formation | Limestone; Dolomitic-limestone | Ma et al. (2022) |
| Fuman | Tarim | 7200–8500 | Middle-Lower Ordovician Yingshan Formation and Yijianfang Formation | Limestone<br>Dolomitic- limestone | Wang et al. (2021c) |
| Tazhong | Tarim | 5500–6800 | Ordovician Yingshan Formation, Yijianfang Formation, and Lianglitage Formation | Reef limestone; Grainstone | Han et al. (2012) |
| Halahatang | Tarim | 5900–7600 | Middle Lower Ordovician Yingshan Formation and Yijianfang Formation | Limestone (Sparite and Micrite) | Zhu et al. (2019) |
| Gucheng | Tarim | 6000–6500 | Middle-Lower Ordovician Yingshan Formation, Yijianfang Formation, Cambrian | Grainstone<br>Dolostone | Cao et al. (2019) |
| Longgang | Sichuan | 5800–7100 | Upper Permian Changxing Formation, Lower Triassic Feixianguan Formation | Reef Limestone | Zhao et al. (2011) |
| Yuanba | Sichuan | 6240–7300 | Upper Permian Changxing Formation, Lower Triassic Feixianguan Formation | Dolostone | Guo et al. (2018) |
| Pengzhou | Sichuan | > 6000 | Middle Triassic Leikoupo Formation | Dolomitic- Limestone; Dolostone | He et al. (2016) |
| Shuangyushi | Sichuan | > 7000 | Middle Permian Qixia Formation | Dolostone | Wen et al. (2021) |
| Laoguanmiao | Sichuan | 7153.5–7175 | Lower Permian Maokou Formation | Limestone | Dai et al. (2021) |
| Puguang | Sichuan | 4776–7100 | Upper Permian Changxing Formation, Lower Triassic Feixianguan Formation | Dolostone | Li et al. (2021b) |
| Keshen | Tarim | 5500–7500 | Lower Cretaceous Bashijiqike Formation | Sandstone | Wang et al. (2013) |
| Bozi-Dabei | Tarim | 5300–7800 | Lower Cretaceous Bashijiqike Formation and Baxigai Formation | Sandstone | Wang et al. (2013) |
| Zhunnan | Junggar | > 7000 | Lower Cretaceous Qingshuihe Formation | Sandstone | Gan et al. (2022) |
| Jianyang | Sichuan | 5140–6660 | Upper Permian Longtan Formation, Lower Permian Maokou Formaton | Basalt<br>Diabase porphyrite | Peng et al. (2022) |

with low porosity and permeability but also leads to heterogeneity in size, spatial arrangement, and connectivity of pores and fractures (Tian et al., 2019; Wang et al., 2020a)—phenomena also found in deep, tectonically complex reservoirs elsewhere (e.g., Wardlaw and Cassan, 1978; Wennberg et al., 2016; Meng et al., 2021).

In multi-cycle superimposed basins, such as the Tarim and Sichuan Basins in China, ultra-deep reservoirs have experienced multi-stage tectonic activities, forming multi-stage and multi-group fractures (Xu et al., 2017). Due to smaller and sparser pores and poor connectivity in host rocks, fractures are important reservoir spaces and dominate flow pathways in ultra-deep reservoirs (Zhao et al., 2020). As the migration channel of diagenetic fluids, fractures are also the key factors affecting the dissolution and transformation of ultra-deep reservoirs (Jia et al., 2021; Lai et al., 2022). Widely developed fractures of various scales connect rocks having isolated pores, enhancing pore connectivity, and improving overall permeability (Odling and Webman, 1991; Odling, 1992; Shi et al., 2022). The fracture-vug systems formed by linked processes of tectonic strain and chemical diagenesis further transform the storage space and may augment the porosity and permeability of ultra-deep reservoirs through dissolution (Baqués et al., 2020; Gong et al., 2020). The mineral fill ratio of fractures in ultra-deep reservoirs varies widely, and research on how such cement deposits may alter flow pathways is key to improving productivity (Liu et al., 2021; Zhang et al., 2021).

In addition to being notably deep, basins in north and west China have been experiencing protracted crustal shortening and—in different places—recent rapid burial and uplift (Thompson et al., 2015). In some basins, geothermal gradients are notably low. Consequently, deep basins and associated fractures in China may differ from those elsewhere where tectonic settings have changed, deep burial may have occurred in the distant past, or geothermal gradients are high. Although a systematic comparison with fractures from other settings is perhaps precipitate, some initial thoughts on such a comparison are provided in a companion paper (Laubach et al., 2023).

Interpreting the origins of fractures is challenging (e.g., Laubach et al., 2019). For those in deeply buried rocks in China, analysis of fracture origins reveals causes that include tectonic, diagenetic, tectonic-diagenetic, and overpressure-related processes (Zeng, 2010). The inference of tectonic origins for many of these fractures is supported in part by the circumstance that the setting of some units, such as Cretaceous deposits, has been continuously in active tectonic settings having broadly consistent kinematics. As is the case elsewhere, the characteristics and distribution of fractures reflect paleotectonic stress and mechanical stratigraphy (Ding et al., 1998; Laubach et al., 2009; Feng et al., 2018; Liu et al., 2020; Mao et al., 2022; Zhang et al., 2021). However, in ultra-deep tight sandstone reservoirs factors influencing fractures are potentially more complex, and additional considerations include the influence of current tectonic movements, how the resulting strain impacts various lithofacies, contemporaneous fluid flow and variable fluid types, and progressive cement accumulations and dissolution (Lander and Laubach, 2015; Lai et al., 2023; Wang et al., 2023a).

Ultra-deep tight sandstone reservoirs are mainly distributed in the foreland thrust belts in western China and are controlled by wide fault-related folds (Wang et al., 2021d; Mao et al., 2022). Different fracture domains develop inside the fault-related folds, controlling the distribution of fractures and the migration and enrichment of oil and gas (Salvini and Storti, 2001; Zu et al., 2013; Mao et al., 2022; Wang et al., 2023b). Effective fractures refer to unfilled (open) fractures contributing to storage space and conductivity; ineffective (sealed or closed) fractures may be barriers to fluid flow (Smart et al., 2001; Laubach et al., 2010; Ravier et al., 2015; Wang et al., 2019a). In tight sandstones and other rocks, the main factors controlling the effectiveness of fractures include diagenesis, overpressure, and present in-situ stress (Zeng and Li, 2009; Laubach et al., 2010; Dong et al., 2018). Due to pervasive overpressure, the effectiveness of fractures in deep sandstones is a determinant of fluid flow (Mao et al., 2020). Owing to overpressure and active tectonic shortening and extension, compared with shallow to medium-depth sandstone reservoirs and those where active tectonics is minimal, the ultra-deep reservoirs in China are likely to contain fractures experiencing long-term dynamic evolution.

## 3. Fracture attributes in ultra-deep tight sandstone reservoirs

### 3.1. Fracture arrays in sandstone

In ultra-deep tight rocks fractures include small faults and opening-mode fractures mainly of tectonic, diagenetic, tectonic-diagenetic, and overpressure origins (Zeng, 2010). The opening can be affected by multiple factors, such as rapid-deep burial, lateral tectonic shortening, and hydrocarbon-generated pressurization (Zeng, 2010; Cobbold et al., 2013; Guo et al., 2016). In ultra-deep sandstones, based on previous research, the main factors correlated with fracture opening include rapid burial or uplift rate, diagenetic overprint potentially increasing strength and brittleness, proximity to larger structures (tectonism), and association with evidence of fluid overpressure (Laubach et al., 2016; Gong et al., 2017; Liu et al., 2021).

Based on their occurrence with respect to mechanical properties (mechanical stratigraphy) and their relationships with layers, most fractures of probable tectonic origin can be further divided into intralayer extension fractures, layer-parallel shear fractures, and transformational shear fractures (Tavani et al., 2011; Zeng et al., 2016; Liu et al., 2021). Intralayer extension fractures are distributed within sandstone layers, aligned perpendicular to and terminating at rock layer interfaces, which may be interbedded finer-grained or shaly material or sandstone bed boundaries. The vertical extent (height) of the intralayer extension fractures is proportional to sandstone thickness dimensions (and degree of interbedding) and is generally small (to c. decimeters), although the bias of sampling fracture height with the vertical core is likely considerable. Despite constrained heights, apertures (opening displacements) may be large (1 to > 2 mm) (Wang et al., 2021b) (Fig. 2a, Table 2).

Fracture spatial arrangement is hard to measure for subvertical fractures with the vertical core. Limited horizontal well data shows that some fractures at least are not regularly spaced, and have marked clustering (e.g., Wu et al., 2023). Nevertheless, core abundance data compared with sandstone layer thickness estimates suggests that for some bed-bound fractures, spacing increases approximately linearly with increasing rock layer thickness (Aguilera and Aguilera, 2001; Zeng and Li, 2009; McDermott et al., 2013).

Layer-parallel shear fractures are formed by interlayer sliding and are apparent from slickensides along bedding planes. Their width is small but readily visible, of order 1 mm (Fig. 2b, Table 2). These fractures are more common in areas with stronger deformation (folding) and larger formation dip angles (Zeng et al., 2016). Transformational shear fractures cut through multiple rock mechanical layers at high dip angles and generally terminate at rock layer interfaces where the lithology and mechanical properties change significantly (Fig. 2c, Table 2). Surfaces of transformational shear fractures are relatively planar. Their widths are usually submillimetric to centimeter-scale, but their vertical extents can reach several meters. Especially in faulted areas, such fractures are denser. The multi-scale characteristics of these fractures are mainly controlled by fold and fault kinematics and mechanical stratigraphy (Zeng et al., 2020).

Away from larger structures, opening-mode fractures are usually ascribed to diagenetic processes or overpressure, and thus may include fractures or transitional origins. Diagenetic fractures are mainly bed-confined and are distributed along bedding. These fractures have a small lateral extent and are characterized by local curvature, bifurcation, or convergence, and may contain vuggy areas that are evidence of dissolution (Fig. 2d, Table 2). Usually, such fractures do not cut through mineral grains but bypass them. The apertures of diagenetic bedding fractures vary from nanometers to micrometers but can reach millimeters where they are filled or dissolved (Fig. 3d, Table 2).

The configurations of bed-parallel fractures imply opening against the load imparted by overburden, a circumstance that can arise owing to overpressure and lateral tectonic loads (e.g., Bons et al., 2012; Cobbold et al., 2013; Gong et al., 2015; Ukar et al., 2017). Stratal uplift caused by tectonic activity is conducive to the expansion and extension of bed-parallel fractures (Zeng et al., 2021).

The formation of intragranular, grain boundary, and transgranular fractures are primarily related to compaction and dissolution during tectonic shortening and diagenesis (Perez and Boles, 2005; Zeng, 2010; Nian et al., 2020) although some transgranular fractures may be the small size fraction of arrays that include larger fractures (e.g., Hooker et al., 2009). Distinguished by their small size and lack of association with large structures, tectonic-diagenetic fractures include intragranular, grain boundary, and transgranular fractures and microfractures. Intragranular fractures located inside mineral grains do not transgress grain boundaries, including cleavages in feldspars and cracks in quartz (Fig. 3b and c, Table 2) whereas grain boundary fractures are along the edges of mineral grains (Fig. 3b and c, Table 2) and transgranular fractures cut across mineral grains and extend beyond grain boundaries. These last are typically wider and longer than intragranular and grain boundary fractures (Fig. 3a, Table 2) (Liu et al., 2021; see also Laubach, 1997). The aperture of transgranular fractures is usually less than 40 μm, while intragranular and grain boundary fractures are less than 20 μm. Although the apertures of intragranular and grain boundary

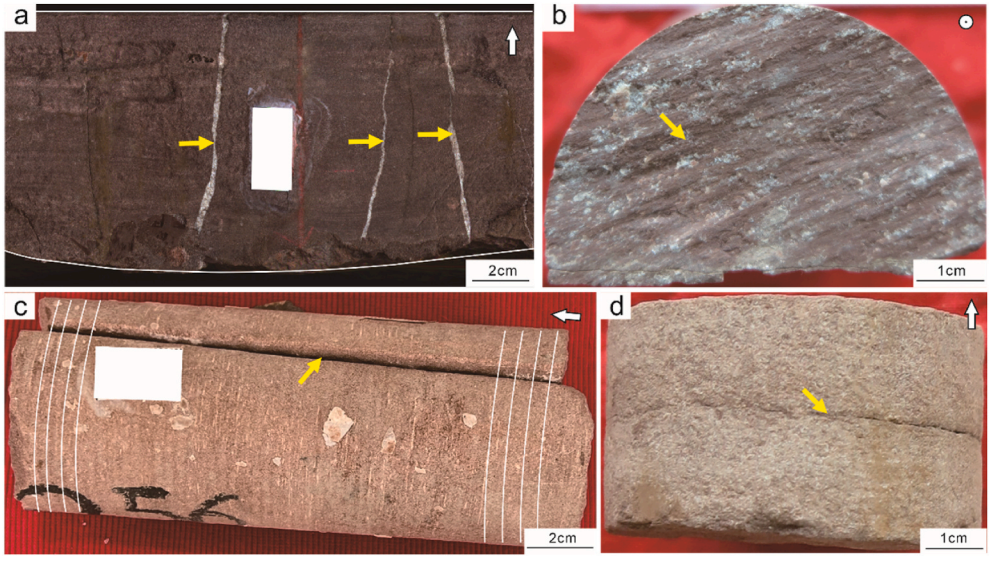


**Fig. 2.** Fractures in cores of the Lower Cretaceous tight sandstones in the Tarim Basin. Arrows indicate fractures. The yellow arrow indicates fractures. White arrow (w) marks the orientation perpendicular to strata, and strata parallel to the photo in Fig. 2b. The white line marks beds). (a) Intralayer extension fractures with high angle and curved surface, completely filled with calcite, Well T-1 in Kelasu Tectonic Belt, Tarim Basin, depth 6506.4m. (b) Layer-parallel shear fracture (fault), partially filled with calcite, Well T-2 in Kelasu Tectonic Belt, Tarim Basin, depth 7008.43m. (c) Transformational shear fracture with high angle and straight surface, unfilled, Well T-3 in Kelasu Tectonic Belt, Tarim Basin, depth 7551.28m. (d) Diagenetic bedding fracture with a straight surface, partially filled with clay minerals, Well T-4 in Kelasu Tectonic Belt, Tarim Basin, depth 6097.3m.

**Table 2**
The ultra-deep fracture types found in China.

| Fracture types | | Distinguished attributes | Reservoirs | Tectonic settings | Distribution areas |
|---|---|---|---|---|---|
| Tectonic fractures | Intralayer extension fractures | Height: cm-dm; Aperture: 1–2 mm | Ultra-deep tight sandstone reservoirs | Foreland thrust belt environment, mainly controlled by fault-related folds | Northern Tarim Basin, Southern Junggar Basin |
| | Layer-parallel shear fractures | Aperture: <1 mm | | | |
| | Transformational shear fractures | Height: dm-m; Aperture: mm-cm | | | |
| Diagenetic fractures | Bed-parallel fractures | Aperture: nm-μm; local curvature | | | |
| Tectonic-diagenetic fractures | Intragranular fractures | Aperture: <20 μm | | | |
| | grain boundary fractures | Aperture: <20 μm | | | |
| | Transgranular fractures | Aperture: <40 μm | | | |
| Overpressure fracture | | Length: >1 cm | | | |
| Tectonic fractures | Intralayer extension fractures | Same attributes as the tight sandstone reservoir | Ultra-deep carbonate reservoirs | Inner cratonic environment, mainly controlled by strike-slip faults | Central Tarim Basin, Central Sichuan Basin |
| | Layer-parallel shear fractures | | | | |
| | Transformational shear fractures | | | | |
| Diagenetic fractures | Bed-parallel fractures | Aperture: μm-mm | | | |
| | Stylolites | Serrated shapes with long extents | | | |
| | Vuggy open fractures | Aperture: μm-cm | | | |
| Tectonic-diagenetic fractures | Tectonic stylolites | Serrated shapes with high height | | | |
| | Tectonic-dissolution fractures | Length: cm-dm | | | |
| | Karst-induced fractures | At the top of the karst caves | | | |

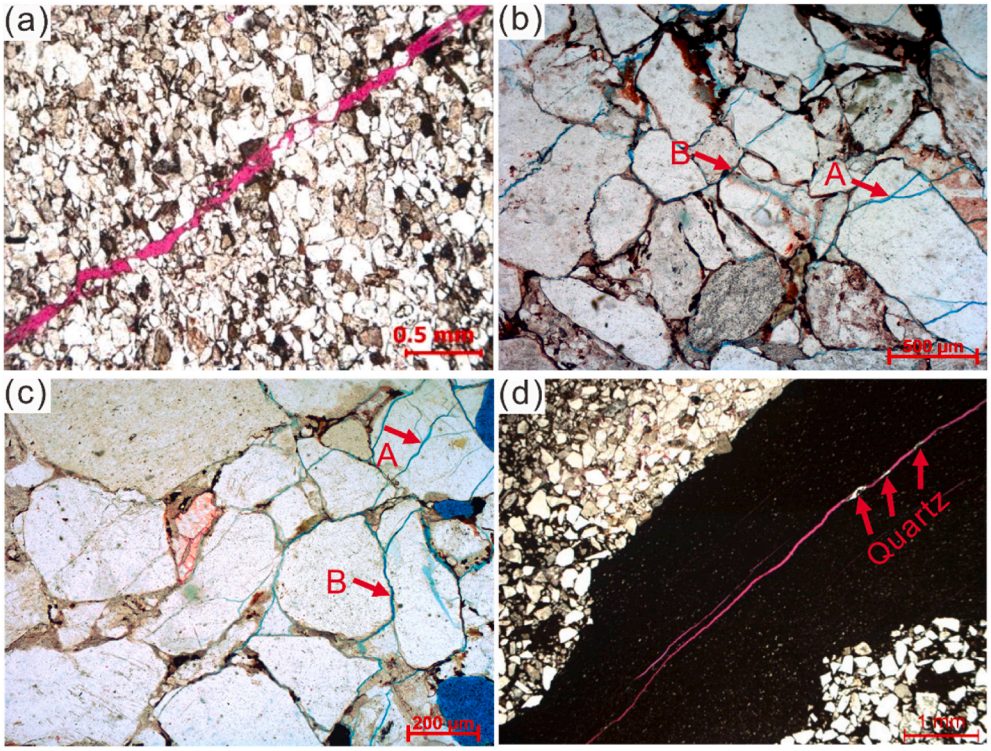


**Fig. 3.** Fractures in thin section, Lower Jurassic and Lower Cretaceous sandstones, Tarim Basin. (a) Transgranular fractures of interpreted tectonic origin with a 0.05 mm aperture, porosity, and partially lined and filled with quartz, Well T-5 in Kelasu Tectonic Belt, Tarim Basin, Lower Cretaceous, depth 7227.33m. (b) Fracture of probable tectonic-diagenetic origin. A, intragranular fractures developed in quartz; B, grain boundary fracture, Well T-6 in Yangxia Depression, Tarim Basin, Lower Jurassic, depth 6068.94m. (c) Fracture of probable tectonic-diagenetic origin. A, intragranular fractures developed in quartz; B, grain boundary fractures, sandstone, Well T-6 in Yangxia Depression, Tarim Basin, Lower Jurassic, depth 6068.94m. (d) Bed-parallel fracture of possible diagenetic origin with a straight surface, partially and sparsely filled with isolated quartz crystals (arrowed), Well T-7 in Kelasu Tectonic Belt, Tarim Basin, Lower Cretaceous, depth 6778.1m.

fractures are relatively small, they connect pores and improve reservoir connectivity, likely benefiting fluid flow in ultra-deep sandstones (Zeng and Li, 2009).

Open microfractures of the type commonly found in deep cores have, elsewhere, been interpreted to be artifacts related to core unloading and handling. Some barren microfractures from ultra-deep cores may have such an origin, but the association of some of these features with cavities related to dissolution, or, locally, minute mineral deposits (Fig. 3), suggests instead that most of these features are representative of the subsurface. Microfractures identical to those in ultra-deep sandstone cores except for being filled with quartz cement, are common in sandstones where the fractures have been subject to longer residence at high temperatures (e.g., Hooker et al., 2009; Anders et al., 2014) and their fill can be explained by gradual quartz accumulation at depth (Lander and Laubach, 2015). Fracture development in settings like the deep Tarim basin, where rapid burial is underway, has geothermal gradients that are

markedly low such that even narrow fractures would not readily fill with quartz (e.g., Lander and Laubach, 2015).

Some fractures exhibiting opening displacement are formed by pore fluid overpressure (Nollet et al., 2005; Boutt et al., 2009; Mourgues et al., 2012). As with all opening-mode fractures, the relative effects of remote tectonic loading and overpressure on opening can be challenging to separate (e.g., Engelder, 1985), particularly in settings like the basins of the west and north China where rapid tectonic shortening and fluid overpressures coincide. Conceptually, the abnormally high-pressure fluid causes the Mohr circle of stress to shift to the left, and when the fluid pressure reaches the failure envelope, the effective minimum principal stress can change from compressive to negative tensile, thus forming overpressure-related fractures (e.g., Zeng et al., 2007). Overpressure-related fractures are mostly filled with calcite, quartz, and other minerals that tie their occurrence to specific points in the burial/thermal history (Zeng, 2010). Because overpressure is presumed to be episodic and shortening continuous, these fractures are interpreted to be primarily caused by overpressure. In contrast to features of primarily tectonic origins, lenticular overpressure-related fractures have sporadic occurrence and are generally short in extent, as little as a few cm). Where present, these fractures can be used to identify past fluid overpressure in sedimentary basins (Zeng et al., 2007; Meng et al., 2017).

Burial and diagenesis affect the development of fractures. The control of composition on fractures is manifested in mineral composition, particle size, and layer thickness (Zeng et al., 2012) and thus mechanical properties and susceptibility to diagenetic change. The higher the content of brittle minerals, the smaller the mineral particles are, and the thinner the rock layer is, the easier it is to develop tectonic fractures (Narr, 1991; Hanks et al., 1997). Diagenesis (such as compaction and cementation) affects the mechanical properties of sandstone by changing its density, porosity, and permeability, thereby controlling the formation of diagenetic and tectonic fractures (e.g., Laubach and Ward, 2006; Lai et al., 2022). In addition, in the burial and evolution of ultra-deep sandstone, with the constant porosity and their brittleness increasing continuously, fractures are favorably formed under tectonic stress (Liu et al., 2021). Tectonism and fluid pressure are the dynamic factors that affect the development of fractures (Zeng et al., 2007; Zeng, 2010; Fall et al., 2015). In different structural positions, the distributions of tectonic stress vary, causing heterogeneous fracture developments. Overpressure caused by fluids is common in ultra-deep and low-porosity strata and facilitates the expansion of early-formed fractures (Zeng, 2010).

### 3.2. Fault-related folds and fractures

Ultra-deep tight sandstone deep wells are mainly in foreland thrust belts, where fault-related folds are widespread. These fault-related folds control these reservoirs' stress and strain history, affecting the fracture distribution (Feng et al., 2018; Zhang et al., 2020b; Wang et al., 2021d; Mao et al., 2022). During fold evolution, fault-related folds experienced complex deformation, such as horizontal shortening and tectonic burial and uplift, forming fracture systems with different occurrences and mechanical properties during multiple periods, patterns which in turn control fluid flow (Suppe, 1983; Suppe and Medwedeff, 1990; Tamara et al., 2015; Li et al., 2018b).

Although folds associated with ultra-deep reservoirs are mainly known from seismic data, folds in the same thrust belts, having similar geometries, as exposed around the basin margins. Although rocks in these folds obviously have different burial histories from those at depth, the outcrop folds have proven useful analogs for reservoirs (e.g., Krézsek et al., 2010; Ogata et al., 2014; Wang et al., 2020a). For some of these outcrops and subsurface targets, the burial and thermal histories coincided until within the last 5 to 10 Ma (e.g., Wei et al., 2023).

Fractures in fault-related folds are the superposed results of regional and local stress fields. Due to the differences in rock deformation and stress fields in different structural positions, fracture distributions in the fault-related fold may be diverse (Smart et al., 2009; Sun et al., 2017; Li et al., 2018b). Where fracture distributions in a certain structural part of a fold are similar from fold to fold, and these specific fold parts can be defined as fracture domains. Fracture domains refer to the area or structural part where fracture occurrences, densities, and scale are consistent or only vary slightly (Salvini et al., 2001; Bazalgette et al., 2010; Mao et al., 2022). According to our discrete element numerical simulations and physical simulations combined with the data from outcrops and cores, regional stress mainly controls the formation of early tectonic fractures in fault-related folds (Tavani et al., 2008; Sun et al., 2017).

With the formation and development of fault-related folds and the increase in slip rate, tectonic fractures evolve over three stages: fracture formation, fracture connection, and new fracture formation (Galuppo et al., 2016). The local stress fields influenced by folds and secondary faults control the fracture development in different structural parts. For example, fault-bend folds in the Lower Cretaceous sandstone within the Tarim basin can be divided into five fracture domains of increasing fracture intensity: an unfolded layer (Fig. 4-A), weakly folded layer within the back limb (Fig. 4-D), core (Fig. 4-C), strongly folded layer within the back limb (Fig. 4-E), and forelimb (Fig. 4-B), and the fracture development degree increases successively (Mao et al., 2022).

Due to the difference in deformation in different zones of the fault-related fold, there are obvious differences in the fracture type, occurrence, and development degree. Fracture domains in limb A did not experience bending or shear and only developed fractures controlled by the regional stress fields. Fracture domains B, C, D, and E were affected by folds and fold-related faults. Fracture domain B is dominated by interlayer slip and layer-parallel shortening and developed interlayer slip-related and layer-parallel shortening-related shear fractures. Fracture domain C was dominated by curvature and interlayer slip and developed curvature-related tensile fractures and interlayer slipping-related shear fractures. Fracture domain D primarily experienced interlayer slip and formed interlayer slip-related shear fractures. Fracture domain E, subject to active hinge parallel shear, interlayer slip, and layer-parallel shortening, developed active hinge parallel shear-related fractures, interlayer slip-related shear fractures, and layer-parallel shortening-related shear fractures (Fig. 4) (Mao et al., 2022).

In ultra-deep tight sandstones of foreland thrust belts, the kinematic characteristics, rock mechanical layers, fault morphology, and structural positions of fault-related folds are the main factors affecting fracture development (Jamison and Pope, 1996; Zeng and Li, 2009; Tamara et al., 2015; Watkins et al., 2015). Fault-related folds in the process of evolution experience many forms of deformation as mentioned in the previous paragraph (Chapple and Spang, 1974; Bazalgette et al., 2010). Especially where plastic detachment layers such as coal and mudstone are developed, conditions are favorable for interlayer slip (e.g., Tanner, 1989; Smart et al., 2009).

## 4. Fracture attributes in ultra-deep carbonate reservoirs

### 4.1. Fracture types and characteristics

Like the ultra-deep tight sandstones, fractures in ultra-deep carbonate rocks mainly include fractures of tectonic, diagenetic, and tectonic-diagenetic origins (He et al., 2019; Méndez et al., 2020). Carbonate rock fractures of tectonic origin have attributes that resemble those in sandstones and are subdivided into intralayer extension fractures (Fig. 5b), transformational shear fractures (Figs. 5a and 6a), and layer-parallel shear fractures (Fig. 5c) (Hausegger et al., 2010; He et al., 2019). Diagenetic fractures in ultra-deep carbonate rocks are abundant and include bed-parallel fractures, stylolites, and vuggy (enhanced dissolution) open fractures (Tondi et al., 2006; Rustichelli et al., 2012; He et al., 2019). The surfaces of bed-parallel fractures are relatively straight, and the apertures are small, ranging from micrometers to millimeters. Most bed-parallel fractures are partially filled with clay

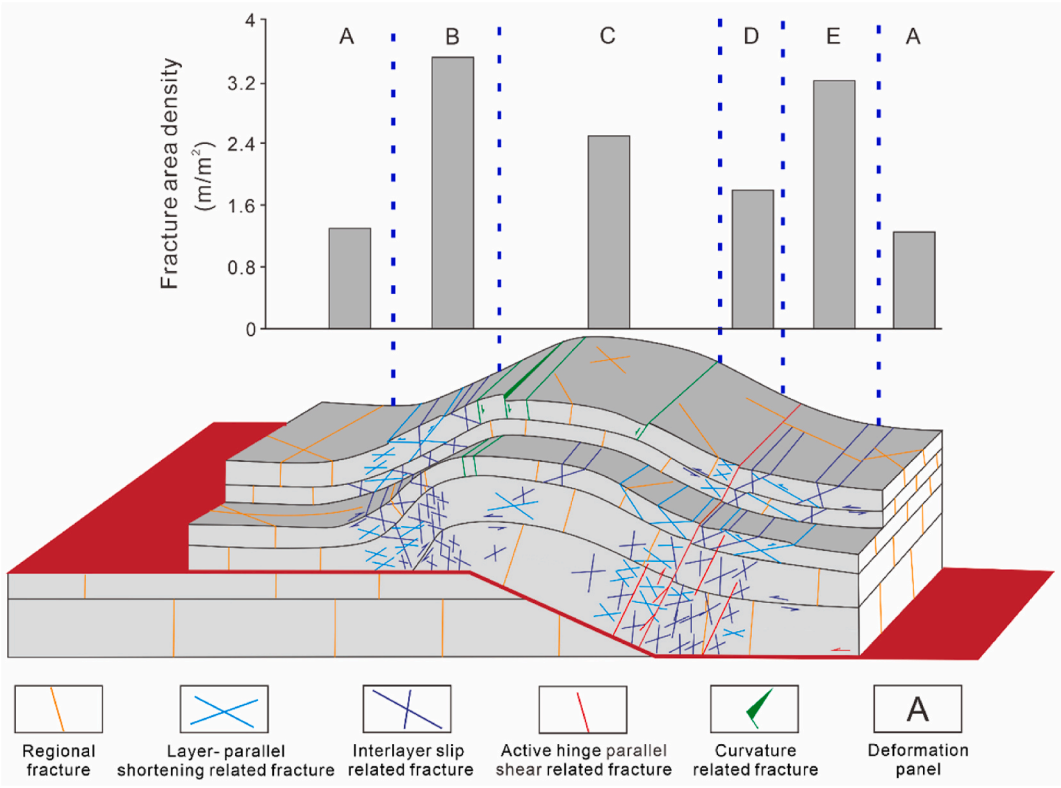


**Fig. 4.** Development model of tectonic fractures controlled by fault-bend fold (After Ma et al., 2022). Domain A is the unfolded layer, developing regional fractures; Domain B is the forelimb, developing interlayer slip-related and layer-parallel shortening-related fractures; Domain C is the fold core, developing curvature-related and interlayer slip-related fractures; Domain D is the weakly folded layer within the back limb, developing interlayer slip related fractures; Domain E is the strongly folded layer within the back limb, developing active hinge parallel shear related fractures, interlayer slip related fractures, and layer-parallel shortening related fractures.

minerals and calcite, and some are fully filled with organic matter (Fig. 5d and 6b). Stylolites along bedding planes have serrated shapes with small apertures and long extents (on the order of core diameter or more). They are fully or partially filled with clay minerals and calcite (Fig. 5e) (Liu and Liu, 2017). The surfaces of dissolution-enhanced open fractures are uneven, and their apertures can range from micrometers to centimeters. Despite a dissolution-enhanced size, these fractures can be fully or partially filled with dolomite, organic matter, and pyrite (Fig. 5f) (Lavoie and Chi, 2001; Li and Xu, 2017).

In ultra-deep carbonate rocks, tectonic-diagenetic tabular structures include stylolites at a high angle to bedding, interpreted to be of tectonic shortening origin and comparable to spaced cleavage in low-grade metamorphic rock. Tectonic stylolites are formed by chemical/pressure dissolution (Railsback et al., 1995; Heap et al., 2014; Zhang et al., 2016). The surface of these structures is serrated, like that of diagenetic stylolites (Fig. 5g). Different from diagenetic stylolites, tectonic stylolites intersect layers at higher angles and develop a larger width of more than 1 mm. Also present are tectonic-dissolution fractures, and karst-induced fractures (He et al., 2019). Tectonic-dissolution fractures are formed by tectonism and pressure dissolution, with short extents of a centimeter to decimeter and characteristics of local fracture networks (Fig. 5h) (Mao et al., 2014). Karst-induced fractures associated with a range of features that indicate the influence of surficial to shallow burial dissolution associated with paleo topography developed in part when karst caves begin to collapse due to the gravity of the overlying strata. Early regional fractures at the top of the karst caves expand further, forming karst-induced fractures. Patterns usually include ring shapes at a range of angles to the top surfaces of caves (Figs. 5i and 6c) (Mao et al., 2014; He et al., 2019).

The main factors controlling fracture development in ultra-deep settings in carbonate rocks include sedimentation, diagenesis, tectonism, and fluid pressure. Sedimentation governs three factors that influence subsequent fracture through their effects on mechanical stratigraphy (e.g., Laubach et al., 2009): mineral composition, fabric, and rock mechanical layer thickness and interface distribution. The main minerals of carbonate rock are dolomite, calcite, and clay minerals. Dolomite has high brittleness and lower compressive strength, and fractures are easily developed where the dolomite content is high (Hood et al., 2004; Guo et al., 2012; Zhao et al., 2018). The main constituents of carbonate rocks are clastic grains and cement. The density of fractures tends to decrease as grain size becomes larger (Ferrill et al., 2017; Ren et al., 2020). If a given mechanical layer has similar rock strength, brittleness, and mechanical properties, for the same loading history fracture abundance and patterns tend to be similar (Rustichelli et al., 2013; Gong et al., 2018). Based on some outcrop observations and models, for the mechanical layer within a specific thickness range, with increasing thickness, the fracture density is expected to decrease, and their height tends to increase (Hobbs, 1967; Narr and Suppe, 1991; Nelson, 2001). The overall high abundance and long trace lengths of nearly vertical fractures in deep cores are not consistent with these models, instead suggesting that at least locally, fracture abundance is higher than what would be expected from the classical mechanical layer/bed thickness relationship. Without the horizontal core, such regular patterns are impossible to corroborate, and some horizontal core data sets suggest that fractures are not regularly spaced at depth, but rather are clustered (e.g., Li et al., 2018c; Wang et al., 2023b). The observations are suggestive rather than definitive and the causes of such variability are conjectural. Lithology may not be uniform in a single layer, in which case there may be differences in rock mechanical properties. Furthermore, early fractures will also affect the mechanical characteristics of the rocks, controlling the formation and distribution of later fractures (Liu et al., 2022). The diagenesis affecting the fracture

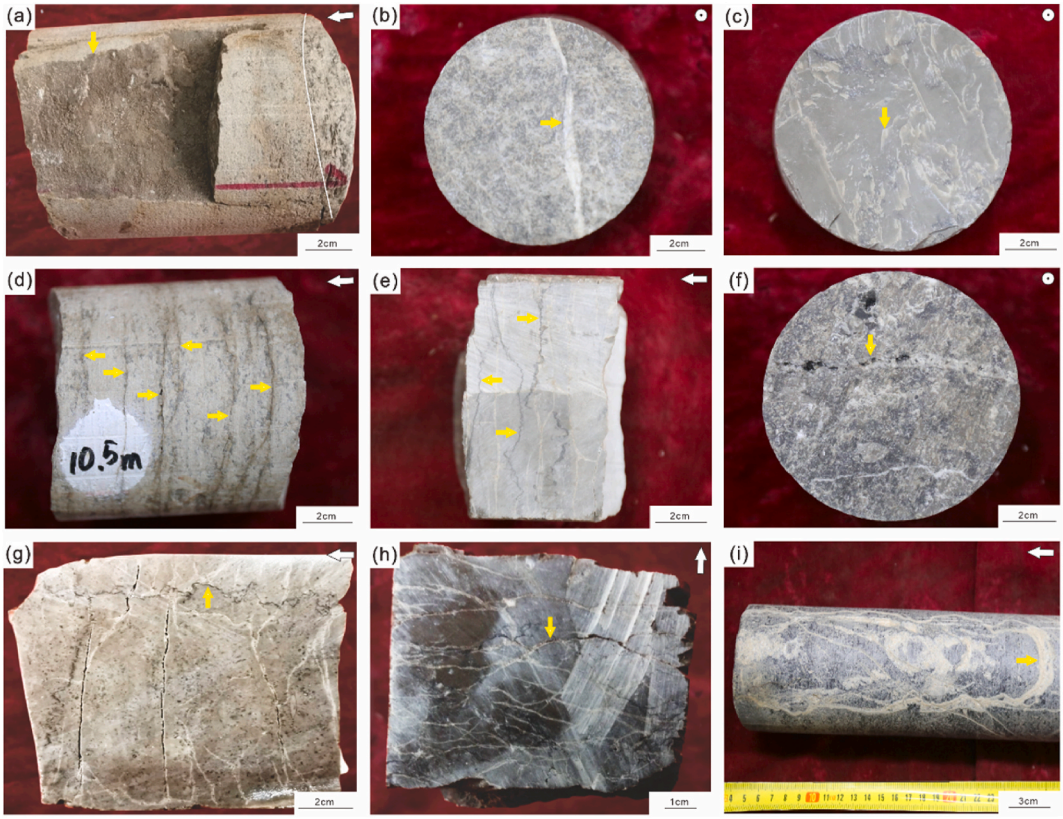


**Fig. 5.** Fractures in cores of the Middle-Lower Ordovician carbonates in the Tarim Basin (Yellow arrow indicates the fractures. White arrow refers to the orientation perpendicular to the strata and the strata parallel to the photo in Fig. 5b, c, and f. White lines refer to beds). (a) Transformational shear fracture with high angle, large extension, and straight surface, partially filled with clay minerals, Well T-8, depth 7428.72m. (b) Intralayer extension fracture with high angle and large aperture, fully filled with calcite, Well T-9, depth 7687.95m. (c) Surface of layer-parallel shear fractures with clear slickenside, unfilled, Well T-10, depth 7787.79m. (d) Diagenetic bed-parallel fractures with relatively straight surfaces and small aperture, partially filled with clay minerals and organic matter, Well T-11, depth 7737.05m. (e) Diagenetic stylolites with small apertures and long extensions in serrated surface, fully filled with clay minerals, Well T-12, depth 7736.4m. (f) Dissolution-enhanced open fractures with uneven surfaces and various aperture, partially filled with calcite, Well T-9, depth 7679m. (g) Tectonic stylolite with high angle and larger aperture in serrated surface, partially filled with clay minerals, Well T-13, depth 7353.2m. (h) Tectonic-dissolution fractures with short extension, local fracture networks develop, partially filled with calcite, Well T-12, depth 7882m. (i) Karst-induced fractures in ring shapes, Well T-14, depth 6469.7m.

development in ultra-deep carbonate rocks mainly includes compaction, cementation, and dissolution (Wu et al., 2019; Yu et al., 2022). During the process of ultra-deep burial, the mechanical compaction of overlying strata and early cementation of brittle minerals make rocks tighter and more prone to fracture (Wu et al., 2018; Ye et al., 2022). Pressure dissolution can provide weak mechanical surfaces, which may be conducive to the further development of fractures (Heap et al., 2014; Baud et al., 2016). In different structural positions, the direction and magnitude of stress vary, resulting in apparent heterogeneity in the occurrences and scales of tectonic fractures (Ding et al., 2012). Where the fluid pressure in pores is much larger than the maximum strength that rocks can resist, extension fractures may develop (Ma et al., 2007, 2010; Cobbold et al., 2013).

### 4.2. Deep-seated cavernous zones in carbonate rocks

Ultra-deep carbonate rocks have diverse fracture types. This diversity is partly determined by the wide range of reactive rock types and mineral compositions of carbonate rocks (He et al., 2019; Liu et al., 2020; Méndez et al., 2020). The core shows abundant evidence of dissolution including stylolites, dissolution-widened open fractures, and fractures having karst-like associations with paleo topography, in contrast with those in sandstones where solution-enhanced structures are rare. In carbonate rocks, structural associations imply processes of compaction, pressure solution, and fluid advection. Together with movements associated with tectonics, these features point to reactive transport as an important factor controlling the development of fractures in this rock type (e.g., Yang et al., 2011; Baqués et al., 2020).

Research has demonstrated that the development of fracture-cavity complexes is a crucial geological feature of ultra-deep carbonate rocks. These cavities control the distribution of favorable reservoirs (e.g., Ukar et al., 2020; Shi et al., 2022). In the Tarim Basin, as exploration progresses, abundant hydrocarbon reserves are still being encountered in carbonate strata buried deeper than 8000 m. This evidence for open pore space (reservoir quality) in carbonate rocks at these prodigious depths is promising that open fractures exist widely under ultra-deep geological conditions (Sun et al., 2013; Zhu et al., 2019; Ma et al., 2022).

In some cases, fault segmentation and across-strike deformation localize fracture development (Kim et al., 2003, 2004; Choi et al., 2016; Wang et al., 2020b; Wu et al., 2021). The history of fracture formation and fracture porosity destruction along such faults can be involved (e.g., Corrêa et al., 2022) and requires combinations of structural quantification and evaluation of mineral deposit geochemistry and age to work out. On the other hand, the occlusion of fractures by cement in these rocks is locally prevalent, possibly to the detriment of the openness of some fractures, promoting reservoir heterogeneity and requiring in-depth evaluation of where open fractures occur (Mao et al., 2014; Yang et al., 2020).

### 4.3. Controls of strike-slip faults on fractures

Fracture-cave reservoirs in carbonate rocks are the primarily high-

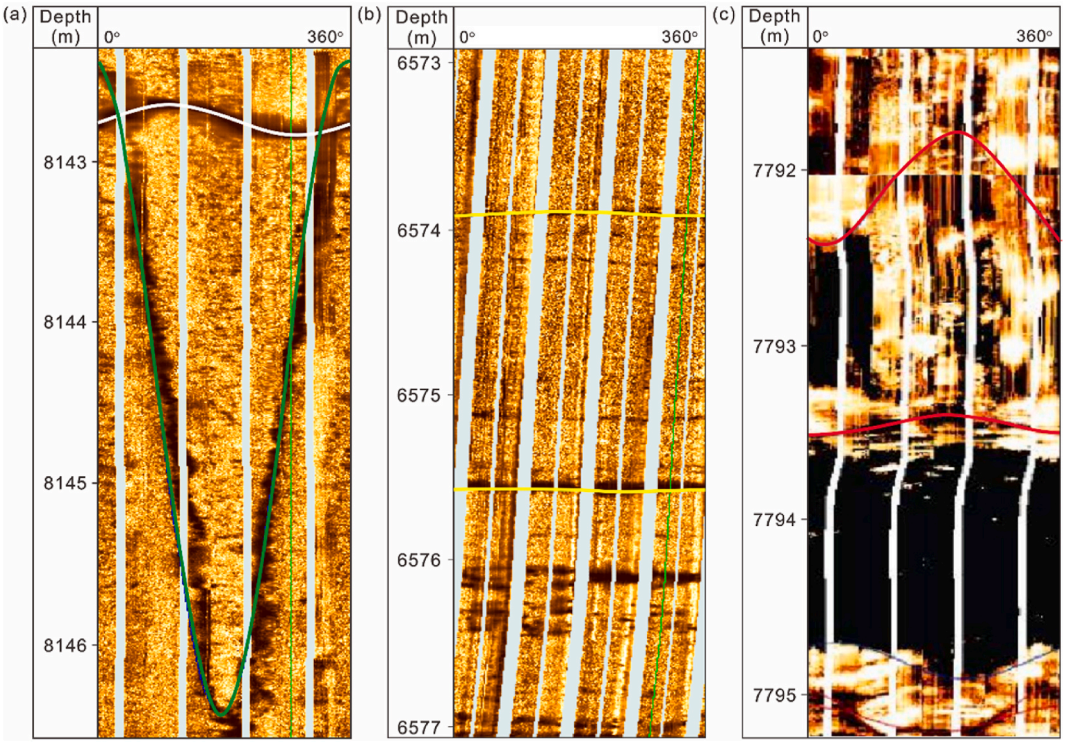


**Fig. 6.** Fracture traces in resistivity image logs of the Lower Ordovician carbonates in the Tarim Basin (Green, yellow, and red lines indicate fractures. White line indicates bedding). (a) Transformational shear fracture with high angle and large vertical extension of several meters, cutting through the upper layer, Well T-12, depth 8143.4–8146.5m. (b) Diagenetic bed-parallel fractures with straight and near horizontal surfaces, Well T-15, depth 6572.9–6577.1m. (c) Karst-induced fractures at different angles developed above karst caves, Well T-16, depth 7791.3–7795.2m (Modified from Ma et al., 2022).

quality reservoirs in China's ultra-deep strata, and in the craton area within the central basin, strike-slip faults control the development of such rocks (Zhao et al., 2020; Li et al., 2021a). In recent years, oil and gas exploration in the ultra-deep Middle-Lower Ordovician carbonate rocks of the Tarim Basin show that high-production wells with cumulative oil production greater than $3 \times 10^4$ tons are primarily distributed along strike-slip faults (Fig. 7a) (Han et al., 2019; Ding et al., 2020; Yang et al., 2020). These strike-slip faults control the distributions of fracture zones, affecting fluid migration and distributions of dissolved pores and caves formed by fluid dissolution (Su et al., 2021; Deng et al., 2022). Fundamentally, fractures and dissolved pores, and caves are the main storage space in ultra-deep carbonate reservoirs. Understanding the

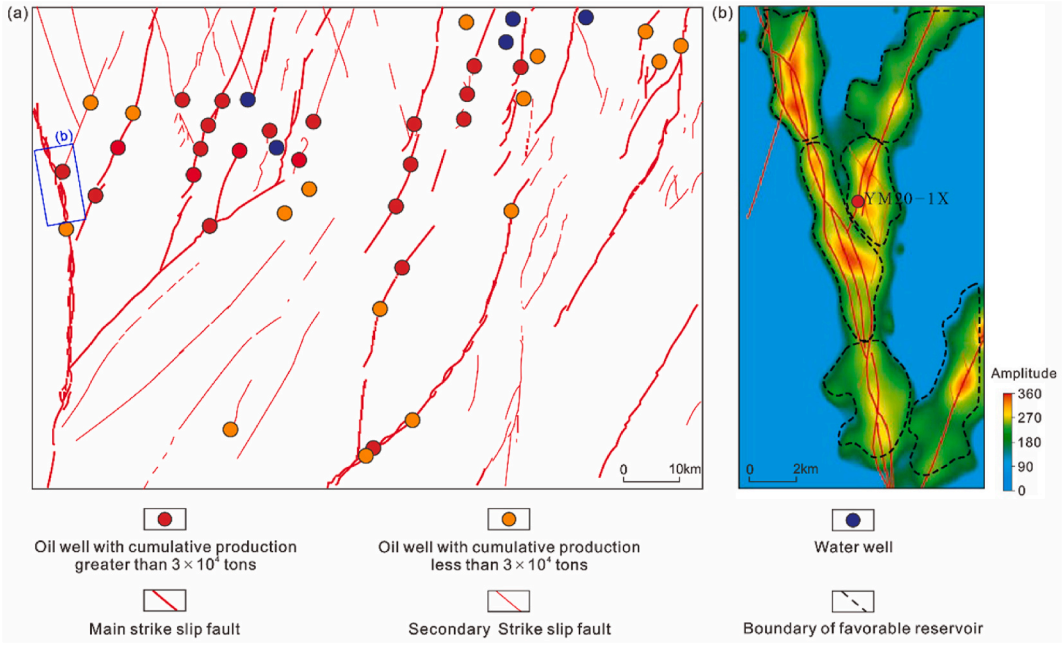


**Fig. 7.** Deep strike-slip faults. (a) Relationship between single-well production and strike-slip faults in ultra-deep carbonate rocks in the Tarim Basin, for location see Fig. 8. (b) Distribution of faults and fractured rocks controlled by strike-slip faults based on 3-D seismic amplitude attributes (All modified from Wang et al., 2021c).

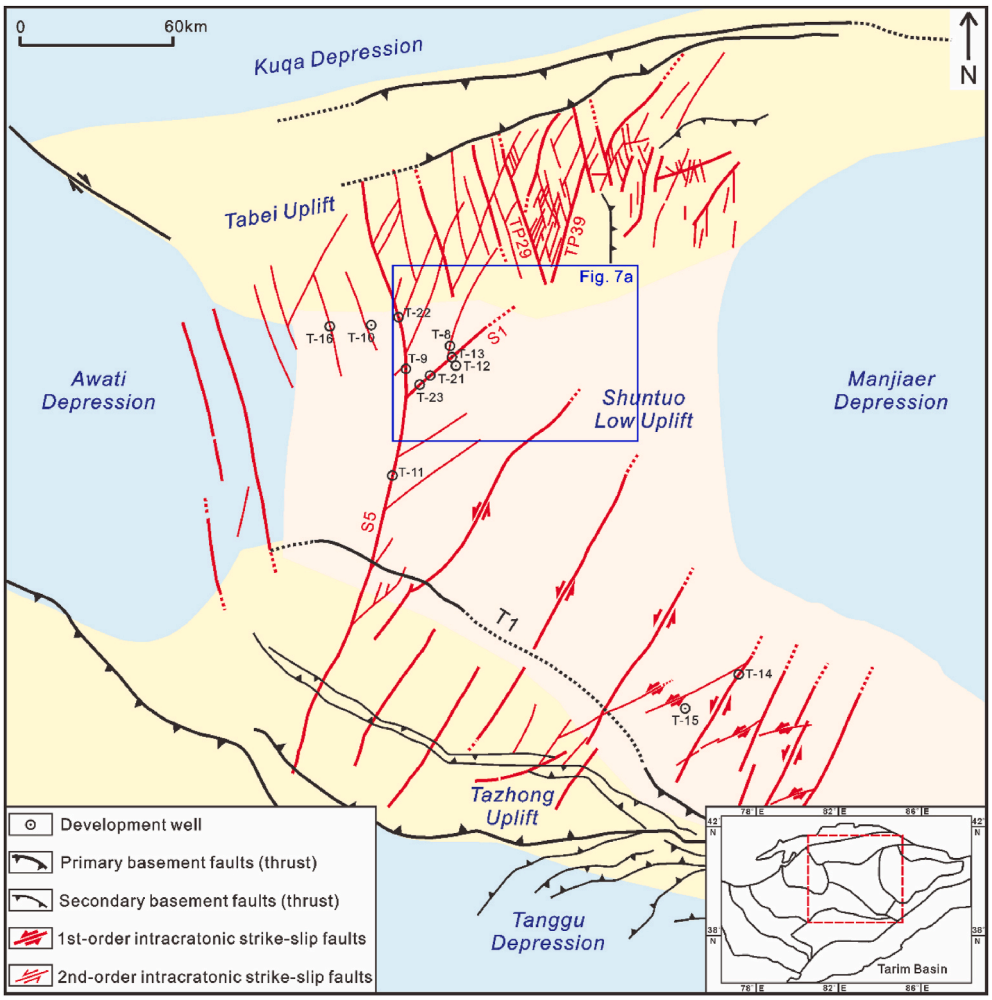


**Fig. 8.** Strike-slip faults in the central and northern Tarim Basin (Modified from Deng et al., 2022). NNE-NNW conjugate strike-slip faults develop in the Tabei Uplift; NNW-SSE and NNE-SSW single-strike strike-slip faults develop in the Shuotuo Low Uplift and north of Tazhong Uplift.

processes controlling dissolution and thus porosity along strike-slip faults on the associated fractures is consequential for guiding the exploration and development of these ultra-deep carbonate rocks.

The ultra-deep strike-slip faults are mainly in the central and northern Tarim Basin, with major strikes being NNE-SSW and NNW-SSE (Han et al., 2017). In the northern Tarim Basin, these are mainly conjugate strike-slip faults, while those in the central Tarim Basin are mainly parallel strike-slip faults (Fig. 8) (Lan et al., 2015). The internal structure of the strike-slip fault is represented by the combination of translation zones, tip zones, and stepover zones (Fig. 9a) (Peacock and Sanderson, 1994; McGrath and Davison, 1995; Kim et al., 2004; Deng et al., 2019; Li et al., 2021a).

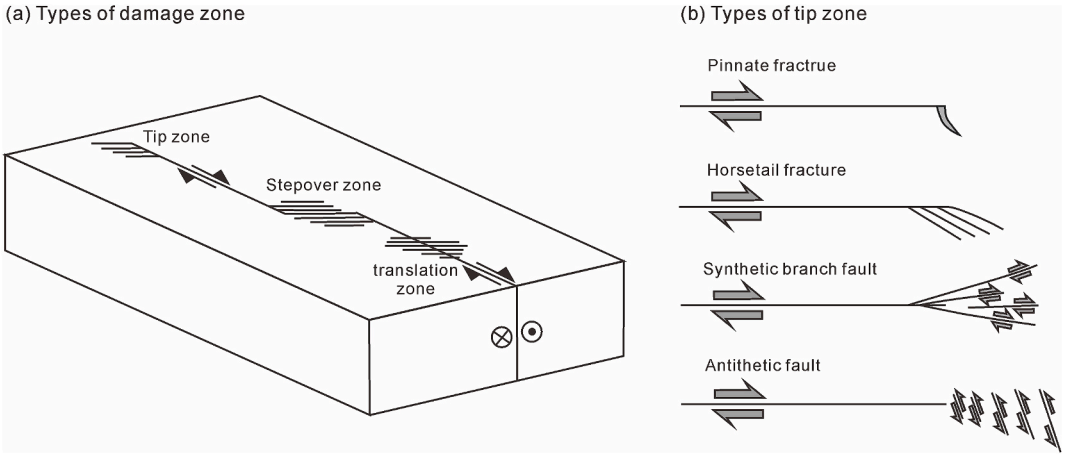


**Fig. 9.** (a) Main damage zones in strike-slip faults. (b) Main fracture types of tip zone (Modified from Kim et al., 2004). Many of these features are inferred to characterize deep carbonate rocks in western and north China.

The translation zones are controlled by the basement strike-slip fault and extend linearly along the main fault with a series of short-extending branch faults. Linear, en echelon, and pinnate structural geometries can be identified in translation zones (Kim et al., 2003, 2004; Han et al., 2017; Wu et al., 2018, 2021). Linear structures usually appear in small faults or areas with weak tectonism and small stress release within the fault. The faults are distributed in parallel with multiple single lines in space, and the tectonic amplitude of strata on both sides is low (Neng et al., 2018; Deng et al., 2019). En-echelon structures show oblique step-like distributions in right or left order on the planes (Han et al., 2017; Neng et al., 2018). Pinnate structures are located on both sides of the main faults, with branch faults distributed symmetrically outward along the main faults and in the shape of feathers (Neng et al., 2018; Deng et al., 2019; Qiu et al., 2022).

The tip zones including pinnate fractures, horsetail fractures, synthetic branch faults, and antithetic faults (Fig. 9b) (Kim et al., 2003, 2004). Among these, pinnate fractures intersect with the main faults at high angles and are characterized by short extents, large apertures, and feather-like opening shapes. Horsetail fractures intersect with the main faults at low angles and are characterized by long extents, small apertures, and bifurcation. Synthetic branch faults are tension faults nearly parallel to the main faults with the same slipping direction. Antithetic faults are distributed in the compressive positions of tip zones and intersect with the main faults at approximately 30° with opposite slip directions (Neng et al., 2018; Qiu et al., 2022).

The stepover zones are the positions where the ends of two translation zones overlap in an en-echelon arrangement (Miller, 1994; Westaway, 1995). Depending on the arrangements on echelon arrangement and slipping directions, the stepover zones can show partially compressive or tensional characteristics (Qi, 2021; Wang et al., 2022b). Where the slip and echelon arrangement directions are opposite, the stepover zones have evidence of shortening and compression. Where the slip and echelon arrangement directions are the same, the stepover zones have extensional characteristics such as open cavities and paleo-topographic depressions. The compressive zone shows back-thrust bulges with long and narrow shapes. The extensional zone forms fault depressions or grabens (Wang et al., 2020b; Bian et al., 2022).

A strike-slip fault can be divided into the fault core and damage zone according to internal structure (e.g., Chester and Logan, 1987; Chester et al., 1993; Caine et al., 1996; Yang, 2015; Choi et al., 2016). The damage zone is the main area where fault-related fractures occur, and within these zones fracture abundance is higher than that of host rocks (e.g., Odling et al., 2004). Within such domains, the expectation is that fracture development degree decreases exponentially with the increase of the distance from the fault core, while beyond this range, the fracture development is mainly controlled by regional deformation (Fig. 7b) (Micarelli et al., 2006; Mitchell and Faulkner, 2009). The widths of the damage zone are closely related to the sizes (scales). Where multiple faults are present, fault-associated deformation may vary with intensities (abundance) of strike-slip faults as zones from adjacent faults amalgamate. As the strike-slip fault's scale and displacement increase, the damage zone's width becomes larger (Fig. 10a and b) (Childs et al., 2009; Ma et al., 2019; Zhao et al., 2021). The fracture development zones of different strata vertically are controlled by the dual factors of the rock mechanics layer and strike-slip fault. In ultra-deep carbonate rocks in Tarim Basin, dolomite, limestone, and sandstone strata are highly brittle layers that tend to have more fractures, while gypsum and mudstone strata are ductile (plastic) layers having lower to no fracture development (Chen et al., 2022).

Strike-slip fault-related fractures are significantly different in abundance pattern and mode in the translation, tip, and stepover zones (Fig. 9a) (Kim et al., 2004). In the translational zones in the middle of the fault, fractures are mainly branch fractures with short extents and are less developed. In the tip zones, fractures are highly developed. The length of pinnate fractures is not as large as those of horsetail fractures, but the pinnate fractures have good connectivity and can form belt-like fracture networks with good porosity and permeability (Kim et al., 2003, 2004; Neng et al., 2018).

Stepover zones between main fault strands (e.g., Peacock, 1991) are another feature common to strike-slip faults in China. In stepover zones, fractures are typically numerous (Wang et al., 2022b). The stepover zones can be divided into hard-linked and soft-linked zones. The hard-linked zones are characterized by mutual fan-like bends and overlaps on the planes. On vertical sections, the two-branch strike-slip faults converge downwards and merge into a single fault, forming a flower structure. Hard-linked zones in stepover zones may have strong stress concentrations and large slip displacements, resulting in wider fracture zones, more fracture strike dispersion, and enhanced fracture connectivity. The soft-linked zones are sub-parallel on the planes and vertical sections, with no physical overlap, small slip displacements, and low fracture development (Wang et al., 2021c). According to the slip direction of both sides and internal stress fields, the stepover zones are divided into push-up and pull-apart stepovers (Liu, 2020; Lyu et al., 2022). The push-up stepovers have complex structures and higher fracture development than the pull-apart stepovers (Kim et al., 2004; Yun, 2021).

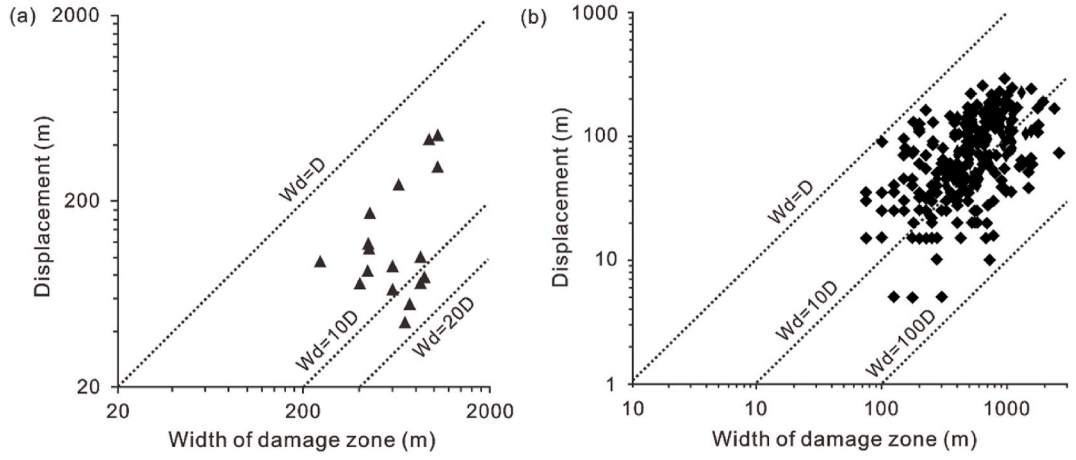


**Fig. 10.** Relationship between the slipping displacement and width of the damage zone of strike-slip faults, northern Tarim Basin (Wd is Width of the damage zone, D is Displacement). (a) S5 strike-slip fault zone in the Shuntuoguole area. Data from Zhao et al. (2021). (b) T1 branch strike-slip fault zones, Tazhong area. Data from Ma et al. (2019).

## 5. Discussion

### 5.1. Formation of ultra-deep fractures

Ultra-deep rocks have experienced long-term burial evolution and multi-period tectonic deformation, resulting in the characteristics of multi-stage fractures (Feng et al., 2018; Li et al., 2021a). In the Tarim Basin according to the analysis of carbon and oxygen isotopes and homogenization temperatures of fluid inclusions of fracture fills correlated with thermal histories, the fractures in ultra-deep sandstones mainly developed at 55 ± 5.7–45 ± 4.3 Ma, 12.2 ± 3.1–7.4 ± 2.6 Ma, and 5.5 ± 1.1–3.8 ± 0.9 Ma (Fig. 11) (Li et al., 2018a). In the Tarim Basin according to U–Pb dating of calcite-filled fractures and the temperature measurements of fluid inclusions, fractures in the Ordovician ultra-deep carbonate rocks mainly formed at 466 ± 11~435.2 ± 9.7 Ma, 391.3 ± 5.5–371 ± 18 Ma, 328.0 ± 9.2–307.6 ± 7.1Ma, and 249.3 ± 2.6–220.5 ± 7.3Ma (Figs. 12 and 13) (Wu et al., 2021; Yang et al., 2021). Combining the formation time of fractures and corresponding burial histories, the burial depths of the ultra-deep strata correspond to the fracture formation time of less than 5000 m (Figs. 11 and 12).

The burial depths corresponding to the fracture formation time of the ultra-deep tight sandstone and carbonate rocks currently explored in China are less than 5000 m. Fractures formed before the reservoir depth reached its maximum (>7000 m). Therefore, fractures in ultra-deep tight rocks developed in a medium-shallow burial environment, like those of conventional low-permeability reservoirs elsewhere. As the strata continue to be buried in the ultra-deep environment, it has been speculated that the main effect is on the capacity of fractures to transmit fluids (effectiveness) through a process of closure, solubilization, and mineral deposit occlusion (Liu et al., 2021; Shi et al., 2022; Xu et al., 2022).

### 5.2. Natural fracture effectiveness in ultra-deep reservoirs

Statistics from macroscopic observation of cores and petrography show that fractures in ultra-deep tight rocks can be filled with calcite, quartz, clay, and other minerals. In the foreland thrust belt of the Kuqa Depression in the Tarim Basin and the southern margin of the Junggar Basin, the proportion of filled fractures in Jurassic ultra-deep sandstone reservoirs is about 35% (Gong et al., 2015; Mao et al., 2020). However, in the Tarim and Sichuan Basins, the proportion of filled fractures in ultra-deep carbonate rocks is about 60% and 70%, respectively (Ding et al., 2012; Mao et al., 2014; Wang et al., 2019a; Yang et al., 2020).

Although oil and gas production are also related to regional source rock characteristics and tectonic activity, we still find a relationship between production and fracture fill ratio. For example, in the Kuqa Depression, tight sandstone intervals with higher fracture fill amounts have lower production. Fully filled fractures have almost no contribution to production (Zhang et al., 2020a), a result found in other basins (Laubach, 2003; Almansour et al., 2020). Consequently, evaluating fracture effectiveness is of significance to ultra-deep reservoirs (Zeng et al., 2012; Baqués et al., 2020; Ukar et al., 2020).

The ability of fractures to conduct and store fluids, or effectiveness, is a function of whether the fractures are open, which in turn is usually considered to depend on the presence of mineral deposits (e.g., Laubach, 2003) or in situ stress (e.g., Finkbeiner et al., 1997). These factors have been attested to deep and ultradeep reservoirs in China (Zeng and Li, 2009; Zhang et al., 2021). According to the fill ratio, fractures are divided into fully filled fractures (veins) and partially or unfilled opening-mode fractures (Laubach, 2003; Laubach and Ward, 2006; Ukar et al., 2019). These fully filled veins are presumed to be ineffective fractures that act as flowing barriers and reduce reservoir quality (e.g., Nelson, 2001; Laubach, 2003; Kuchuk et al., 2015). The partially and unfilled opening-mode fractures may be effective and act as channels and storage spaces for oil and gas (e.g., Laubach et al., 2010; Ravier et al., 2015), but the effectiveness of such fractures for augmenting reservoir performance is challenging to assess since other fracture system attributes may govern fluid flow. Among these other attributes are aperture and aperture distribution (e.g., Klimczak et al., 2010), length distribution (e.g., Philip et al., 2005), connectivity (e.g., Sanderson and Nixon, 2015), and the effects of diagenesis in reducing connectivity (Forstner and Laubach, 2022). In addition, fractures with larger apertures may be more effective, providing more storage space and contributing to greater permeability (Liu et al., 2021; Zhang et al., 2021; Mejia et al., 2022). For example, in a study of the effectiveness of ultra-deep fractures in the Kuqa Depression, it was found that the greater the fracture aperture, the higher the daily oil production of related reservoir intervals (Xu et al., 2022).

Compared with shallow reservoirs, ultra-deep reservoirs have the characteristics of high temperature and high pressure. For example, in Kuqa Depression, the burial depth of ultra-deep tight sandstones commonly exceeds 6000m. The temperature generally exceeds 130 °C

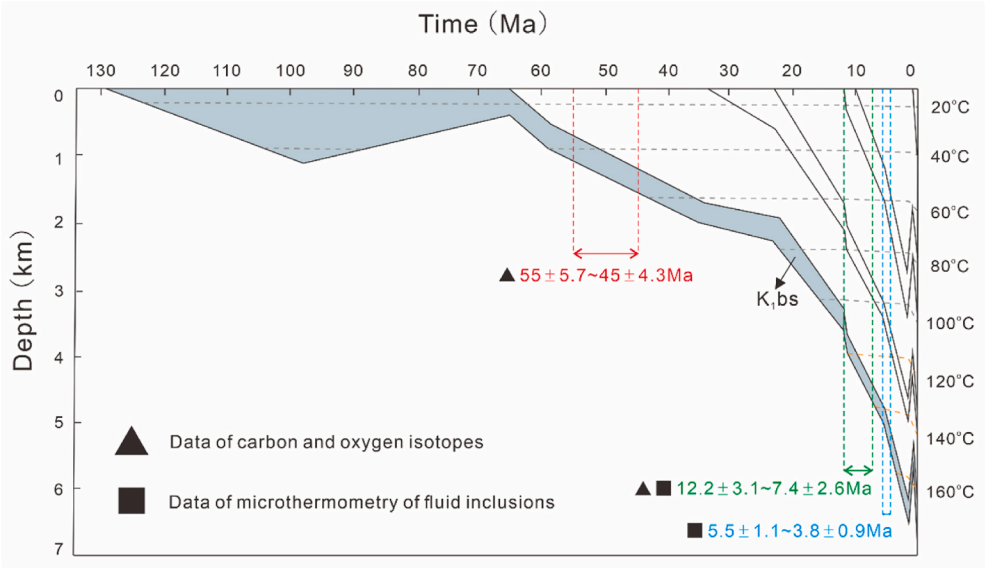


**Fig. 11.** Burial history curve and formation time of fractures of the Lower Cretaceous Bashijiqike Sandstone Formation ($K_1bs$), northern Tarim Basin. Data on carbon and oxygen isotope and fluid inclusion homogenization temperature in calcite deposits in fractures from Li et al. (2018a).

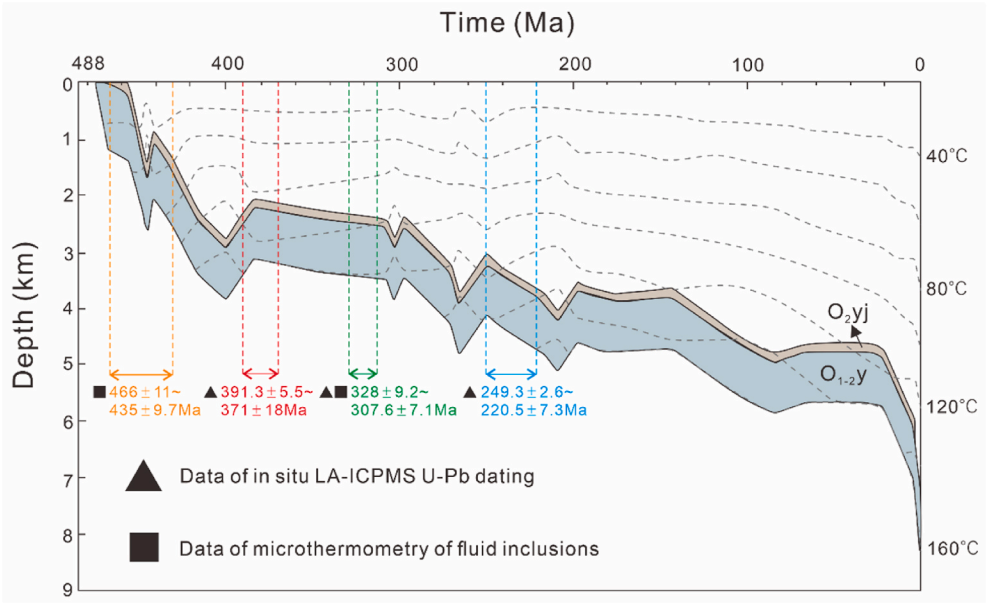


**Fig. 12.** Burial history curve and formation time of fractures of Middle-Lower Ordovician Yijianfang ($O_2yj$) and Yingshan Carbonate Formation ($O_{1\text{-}2}y$), northern Tarim Basin. In-situ LA-ICPMS U–Pb isotope age data in calcite deposits in fractures from Jia (2019). Data on fluid inclusion homogenization temperatures in calcite deposits in fractures from Wang et al. (2022a).

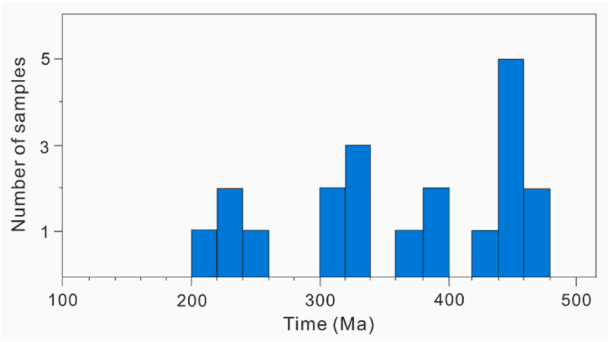


**Fig. 13.** U–Pb isotopic dating of calcite-filled fractures (veins) associated with strike-slip faults in Middle-Lower Ordovician Yijianfang ($O_2yj$) and Yingshan Carbonate Formation ($O_{1\text{-}2}y$), northern Tarim Basin. Data from Wang et al. (2021a) and Wu et al. (2021).

and formation pressure exceeds 90 MPa. The pressure coefficient generally exceeds 1.6 and is positively correlated with the burial depth, showing widespread overpressure (Guo et al., 2016). At higher temperatures, cement accumulation is more rapid, tending to cause fractures to fill and their effectiveness to decrease. On the other hand, some types of cement, like quartz, accumulate slowly even at temperatures above 170 °C, such that open fractures can persist at great depth for millions of years (Laubach et al., 2019). Other chemical reactions, such as calcite precipitation, are more sensitive to fluid chemistry, and calcite deposits in sandstone fracture are highly variable at a wide range of depths (e.g., Weisenberger et al., 2019). The competitive relationships between the rates of fracture opening and mineral cement accumulation—the ratio of mineral cement thickness normal to the fracture wall to accumulation time (Gale et al., 2010; Lander and Laubach, 2015) may determine if fractures remain open. Moreover, mineral bridges (partial fracture occlusion) formed during fracture opening (Lander and Laubach, 2015; Fall et al., 2016; Ukar and Laubach, 2016; Wang et al., 2021d) may effectively support the fracture spaces under compressive stress and preserve fracture openness (effectiveness) (e.g., Laubach et al., 2004a).

Where the mineral composition of the matrix rock is approximately the same, the mineral type within fractures also affects fracture effectiveness in ultra-deep rocks. Calcite is more brittle and fractured calcite (for example in fault zones) is accessible to corrosive acidic fluids that tend to dissolve them. Such a process occurs more readily in calcite than anhydrite. Therefore, fractures filled with calcite can be re-opened after dissolution by transient fluids and may regain effectiveness, while fractures filled with anhydrite are more effective seals due to their good stability (Wang et al., 2020a). In basins such as the Tarim regional mixing of meteoric water in elevated areas such as the Tien Shan along partly porous faults that breach the surface with deep-seated migrating sulfur-rich oil is a potential cause of such reactions (e.g., Baqués et al., 2020) that needs to be studied by basin-scale reactive transport models.

To illustrate some effects of reactive mineral deposits in fractures, consider the KS area of the Kuqa Depression in Tarim Basin, where fractures in Well T-17 at depths of 6890–6976 m are mainly filled with calcite. Gas production before acidification is $3 \times 10^4$ $m^3$/d, and after, it is $41 \times 10^4$ $m^3$/d, demonstrating that acidification significantly increased the gas production. The fractures in Well T-18 at depths of 6953–7062 m are mainly filled with anhydrite. Gas production before acidification is $30.2 \times 10^4$ $m^3$/d, and after, it is $31.1 \times 10^4$ $m^3$/d, showing the gas production is almost unchanged. Therefore, fractures filled with calcite are more likely to transform into effective fractures in later periods than those filled with anhydrite (Wang et al., 2021a).

After fractures are formed or filled, dissolution may cause the formation of dissolution pores, so formerly sealed fractures may become conduits (Liu et al., 2005; Wang et al., 2022a). Evidence from ultra-deep core suggests that strong dissolution can make fractures more effective (Liu et al., 2016). Additionally, late tectonic uplift and denudation can re-open the early-filled fractures and restore their effectiveness (Zeng et al., 2012) or subject them to corrosive fluid regimes.

In ultra-deep reservoirs overpressure formed by uneven compaction and tectonic compression is common, which is a key to maintaining the good effectiveness of ultra-deep fractures (Berthelon et al., 2021; Zeng et al., 2004; Guo et al., 2016). For example, in the Kuqa Depression of the Tarim Basin overpressure is common and the pressure coefficient is above 1.7, suggesting that overpressure could be a factor for retaining fracture effectiveness (Gong et al., 2015). Overpressure tends to reduce normal stress on the fracture surfaces and increases the aperture to make them more effective (Dong et al., 2018). In the same set of fractures, the

fill ratio of these fractures with smaller apertures is higher, and their effectiveness is poorer, as in other areas (e.g., Laubach et al., 2004b). In other words, the smaller fractures do not contribute to permeability enhancement because they are filled.

Cement deposits accumulated in fractures or host rocks may stiffen fractures such that they resist closure under ambient loads (e.g., Olson et al., 2007, their Fig. 2), but for those created in the near-contemporaneous stress field where little cement has accumulated in host rock or fractures, fractures can be expected to be compliant. Where fractures are compliant, they may differ in their effectiveness depending on in situ stress conditions (Fig. 14). In this case, fractures parallel to the orientations of the current maximum horizontal principal stress have the smallest normal stress on their surfaces, resulting in a tendency to larger apertures and (potentially) greater effectiveness. However, planes perpendicular to the current maximum horizontal principal stress have the largest normal stress on their surfaces, thus they will tend to be small in aperture and poor in effectiveness. Fractures oblique to the present maximum horizontal principal stress have moderate aperture and effectiveness (e.g., Finkbeiner et al., 1997; Zeng and Li, 2009; Liu et al., 2021).

For example, in Well T-19 of the Kuqa Depression in Tarim Basin, the fracture linear density is 0.21/m at a depth of 6737–6950 m, and the normal stress on these fracture surfaces is 45 MPa. This well has a daily gas production of $10 \times 10^4$ $m^3$/d. The linear fracture density of Well T-20 at a depth of 7016–7117 m is 0.25/m, and the normal stress on the fracture surfaces is 36.8 MPa. In contrast, the daily gas production of this well is $30.9 \times 10^4$ $m^3$/d. This is compatible with the partial closure of compliant fractures and less normal stress on the fracture surface correlating with more effective fluid flow and thus higher single-well daily production (Xu et al., 2022). For fractures with the same strikes, the normal stress on the high-angle fracture surface is smaller than that on the low-angle or horizontal fracture surface, so high-angle fractures could have greater apertures and better effectiveness (Lai et al., 2021).

During the process of oil and gas reservoir development, the effectiveness of fracture zones controlled by ultra-deep strike-slip faults is correlated to the present in-situ stress. When the fault trending is parallel to or intersects with the current stress direction at a small angle, the opening ability and effectiveness of fault-controlled fractures are the best. When the intersecting angle is large, the opening ability and effectiveness are the worst. For example, the orientation of the present maximum horizontal principal stress in the central and northern Tarim Basin is NNE-SSW (Huang et al., 2022). The opening ability and effectiveness of fracture zones associated with NNE-SSW trending strike-slip faults are markedly better than those with NNW-SSE trending strike-slip faults. For example, in the TP39-TP29 conjugate strike-slip fault systems

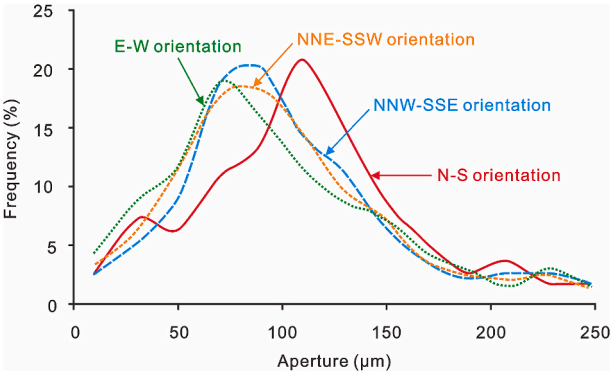


**Fig. 14.** The aperture distribution of natural fractures with different strikes based on image logs in the Lower Cretaceous tight sandstones in the Kuqa Depression, Tarim Basin (N = 658). (a) S–N orientation (N = 112). (b) NNW-SSE orientation (N = 231). (c) NNE-SSW orientation (N = 246). (d) E-W orientation (N = 69). The current orientation of in-situ maximum stress is north-south). Data from Liu et al. (2021).

of the TP area in Tarim Basin, the single-well daily oil production in the fracture zones associated with NNE-SSW trending strike-slip faults is generally greater than $1.5 \times 10^4$ t, while that with NNW-SSE trending strike-slip faults is generally less than $0.5 \times 10^4$ t (Deng et al., 2022).

Fracture effectiveness in different positions within the same strike-slip faults also presents apparent contrasts. The fracture effectiveness in the stepover zones is significantly higher than in the translation zones (Deng et al., 2022). For the stepover zones, fractures have higher development in the push-up stepover than the pull-apart stepover. However, fractures in push-up stepover have smaller apertures and their effectiveness and connectivity are poorer compared to pull-apart stepover, which is not conducive to a high and stable yield (Wang et al., 2022b). For example, in the southern S1 strike-slip fault of the SB area in Tarim Basin, Well T-21, which penetrates the pull-apart stepover, has an average oil production per unit pressure drop of 2147 t/MPa. In the southern S5 strike-slip fault, the Well T-22, which passes through the push-up stepovers, has an average oil production per unit pressure drop of 1357 t/MPa. While in the northern S1 strike-slip fault, the Well T-23, which encountered the translation zone, has an average oil production per unit pressure drop of 885 t/MPa (Liu et al., 2020; Deng et al., 2022). These figures indicate that the oil production and effectiveness of fractures in the stepover zones are significantly higher than those in the translation zones. Oil production and effectiveness of fractures in the pull-apart stepovers are higher than in the push-up stepovers. Consequently, the diversities of fracture effectiveness for different trending faults and stepover zones inside the fault zone lead to apparent variabilities in oil and gas production. The high-productivity wells are more likely to be located in the pull-apart stepovers within strike-slip faults that intersect parallel or at small angles to the direction of present in-situ stress (Deng et al., 2022).

## 6. Conclusions

(1) Ultra-deep reservoirs with burial depths of more than 6000 m are essential fields for China oil and gas exploration and are mainly focused on the sandstone reservoirs in the Kuqa Depression of the Tarim Basin and the central and southern Junggar Basin and the carbonate reservoirs in the Tarim and Sichuan Basins. Ultra-deep rocks widely developed natural fractures are the main storage space and flow pathways in these reservoirs, influencing oil and gas enrichment and single-well production.

(2) In ultra-deep reservoirs fractures mainly have tectonic, diagenetic, tectonic-diagenetic, and overpressure origins. In contrast to the ultra-deep reservoirs found in various nations, the distribution of China's ones is predominantly influenced by fault-related folds and strike-slip faults. Fault-related folds affect the fracture distribution of ultra-deep tight sandstone reservoirs in the foreland thrust belt, which is divided into five fracture domains. The scale, structural style, and linkage evolution of strike-slip faults control the fracture distribution for these carbonate rocks. Moreover, there are notable variations in fracture development characteristics in different structural positions.

(3) Ultra-deep rocks have fractures that developed in multiple periods. We infer that some of these fractures formed when rocks were buried at depths less than 5000m. The increase in burial depth after the formation of fractures primarily influences their effectiveness (mainly seepage capacity). Fracture-forming processes include overpressure, present in situ, and tectonic loading. Other variables modifying fractures include when fractures formed (timing), regional and local structural position, and scale and fluid flow leading to heterogeneity in whether fractures are mineral filled, open, or enhanced by dissolution. They all cause heterogeneities in oil and gas production.

## Declaration of competing interest

The authors declare that they have no known competing financial interests or personal relationships that could have appeared to influence the work reported in this paper.

## Data availability

The data that has been used is confidential.

## Acknowledgments

This paper is supported by the National Natural Science Foundation of China (No. U21B2062). We greatly acknowledge the researchers of the data and figures cited in this paper, which provide ample evidence for the conclusions made in our study. We are particularly grateful to JSG editors Dr. Stephen E. Laubach, Dr. John Hooker, and Dr. Qiqi Wang, and anonymous reviewers for their constructive comments, which contributed significantly to the paper.

## References

Aguilera, R., Aguilera, M.S., 2001. Well test analysis of multi-layered naturally fractured reservoirs with variable thickness and variable fracture spacing. J. Can. Petrol. Technol. 40 (12) https://doi.org/10.2118/01-12-TN2. Petsoc–01–12–Tn2.

Almansour, A., Laubach, S.E., Bickel, J.E., Schultz, R.A., 2020. Value of Information analysis of a fracture prediction method. SPE. Reserv. Eval. Eng. 23 (3), 811–823. https://doi.org/10.2118/198906-PA.

Anders, M.H., Laubach, S.E., Scholz, C.H., 2014. Microfractures: a review. J. Struct. Geol. 69, 377–394. https://doi.org/10.1016/j.jsg.2014.05.011. Part B.

Baqués, V., Ukar, E., Laubach, S.E., Forstner, S.R., Fall, A., 2020. Fracture, dissolution, and cementation events in ordovician carbonate reservoirs, Tarim Basin, NW China. Geofluids 2020, 9037429. https://doi.org/10.1155/2020/9037429.

Barker, C., Takach, N.E., 1992. Prediction of natural gas composition in ultradeep sandstone reservoirs. AAPG Bull. 76 (12), 1859–1873. https://doi.org/10.1306/BDFF8B00-1718-11D7-8645000102C1865D.

Baud, P., Rolland, A., Heap, M., Xu, T., Nicolé, M., Ferrand, T., Reuschlé, T., Toussaint, R., Conil, N., 2016. Impact of stylolites on the mechanical strength of limestone. Tectonophysics 690, 4–20. https://doi.org/10.1016/j.tecto.2016.03.004.

Bazalgette, L., Petit, J.P., Amrhar, M., Ouanaïmi, H., 2010. Aspects and origins of fractured dip-domain boundaries in folded carbonate rocks. J. Struct. Geol. 32, 523–536. https://doi.org/10.1016/j.jsg.2010.03.002.

Berthelon, J., Brüch, A., Colombo, D., Frey, J., Traby, R., Bouziat, A., Cacas-Stentz, M.C., Cornu, T., 2021. Impact of tectonic shortening on fluid overpressure in petroleum system modelling: insights from the Neuquén basin, Argentina. Mar. Petrol. Geol. 127, 104933 https://doi.org/10.1016/j.marpetgeo.2021.104933.

Bian, Q., Deng, S., Lin, H., Han, J., 2022. Strike-slip salt tectonics in the Shuntuoguole low uplift, Tarim Basin, and the significance to petroleum exploration. Mar. Petrol. Geol. 139, 105600 https://doi.org/10.1016/j.marpetgeo.2022.105600.

Bons, P.D., Elburg, M.A., Gomez-Rivas, E., 2012. A review of the formation of tectonic veins and their microstructures. J. Struct. Geol. 43, 33–62. https://doi.org/10.1016/j.jsg.2012.07.005.

Bosworth, W., Huchon, P., McClay, K., 2005. The red sea and gulf of aden basins. J. Afr. Earth Sci. 43 (1–3), 334–378. https://doi.org/10.1016/j.jafrearsci.2005.07.020.

Boutt, D.F., Goodwin, L., McPherson, B.J., 2009. Role of permeability and storage in the initiation and propagation of natural hydraulic fractures. Water Resour. Res. 45 (5), 1–18. https://doi.org/10.1029/2007WR006557.

Caine, J.S., Evans, J.P., Forster, C.B., 1996. Fault zone architecture and permeability structure. Geol. 24, 1025–1028. https://doi.org/10.1130/0091-7613(1996)024<1025:FZAAPS>2.3.CO;2.

Cao, Y.H., Wang, S., Zhang, Y.J., Yang, M., Yan, L., Zhao, Y.M., Zhang, J.L., Wang, X.D., Zhou, X.X., Wang, H.J., 2019. Petroleum geological conditions and exploration potential of lower paleozoic carbonate rocks in gucheng area, Tarim Basin, China. Petrol. Explor. Dev+. 46 (6), 1165–1181. https://doi.org/10.1016/S1876-3804(19)60271-5.

Chapple, W.M., Spang, J.H., 1974. Significance of layer-parallel slip during folding of layered sedimentary rocks. Geol. Soc. Am. Bull. 85, 1523–1534. https://doi.org/10.1130/0016-7606(1974)85<1523:SOLSDF>2.0.CO;2.

Chen, J., He, D., Tian, F., Huang, C., Ma, D., Zhang, W., 2022. Control of mechanical stratigraphy on the stratified style of strike-slip faults in the central Tarim Craton, NW China. Tectonophysics 830, 229307. https://doi.org/10.1016/j.tecto.2022.229307.

Chester, F.M., Evans, J.P., Biegel, R.L., 1993. Internal structure and weakening mechanisms of the San Andreas fault. J. Geophys. Res. 98, 771–786. https://doi.org/10.1029/92JB01866.

Chester, F.M., Logan, J.M., 1987. Composite planar fabric of gouge from the Punchbowl Fault, California. J. Struct. Geol. 9, 621–634. https://doi.org/10.1016/0191-8141(87)90147-7.

Childs, C., Sylta, Ø., Moriya, S., Morewood, N., Manzocchi, T., Walsh, J.J., Hermanssen, D., 2009. Calibrating fault seal using a hydrocarbon migration model of the Oseberg Syd area, Viking Graben. Mar. Petrol. Geol. 26, 764–774. https://doi.org/10.1016/j.marpetgeo.2008.05.004.

Choi, J.H., Edwards, P., Ko, K., Kim, Y.S., 2016. Definition and classification of fault damage zones: a review and a new methodological approach. Earth Sci. Rev. 152, 70–87. https://doi.org/10.1016/j.earscirev.2015.11.006.

Cobbold, P.R., Zanella, A., Rodrigues, N., Løseth, H., 2013. Bedding-parallel fibrous veins (beef and cone-in-cone): worldwide occurrence and possible significance in terms of fluid overpressure, hydrocarbon generation and mineralization. Mar. Petrol. Geol. 43, 1–20. https://doi.org/10.1016/j.marpetgeo.2013.01.010.

Corrêa, R.S.M., Ukar, E., Laubach, S.E., Aubert, I., Lamarche, J., Wang, Q., Stockli, D., Stockli, L., Larson, T., 2022. Episodic reactivation of carbonate fault zones with implications for permeability – an example from Provence, Southeast France. Mar. Petrol. Geol. 145, 105905 https://doi.org/10.1016/j.marpetgeo.2022.105905.

Dai, J., Ni, Y., Liu, Q., Wu, X., Gong, D., Hong, F., Zhang, Y., Liao, F., Yan, Z., Li, H., 2021. Sichuan super gas basin in southwest China. Petrol. Explor. Dev+. 48, 1251–1259. https://doi.org/10.1016/S1876-3804(21)60284-7.

Deng, S., Li, H., Zhang, Z., Zhang, J., Yang, X., 2019. Structural characterization of intracratonic strike-slip faults in the central Tarim Basin. AAPG Bull. 103, 109–137. https://doi.org/10.1306/06071817354.

Deng, S., Zhao, R., Kong, Q., Li, Y., Li, B., 2022. Two distinct strike-slip fault networks in the Shunbei area and its surroundings, Tarim Basin: hydrocarbon accumulation, distribution, and controlling factors. AAPG Bull. 106, 77–102. https://doi.org/10.1306/07202119113.

Ding, W., Fan, T., Yu, B., Huang, X., Liu, C., 2012. Ordovician carbonate reservoir fracture characteristics and fracture distribution forecasting in the Tazhong area of Tarim Basin, Northwest China. J. Petrol. Sci. Eng. 86– 87, 62–70. https://doi.org/10.1016/j.petrol.2012.03.006.

Ding, Z.Y., Qian, X.L., Huo, H., Yang, L.Q., 1998. A new method for quantitative prediction of structural fractures: binary method. Oil Gas Geol. 19 (1), 1–14. https://doi:10.11743/ogg19980101.

Ding, Z.W., Wang, R.J., Chen, F.F., Yang, J.P., Zhu, Z.Q., Yang, Z.M., Sun, X.H., Xian, B., Li, E.P., Shi, T., Zuo, C., Li, Y., 2020. Origin, hydrocarbon accumulation and oil-gas enrichment of fault-karst carbonate reservoirs: a case study of Ordovician carbonate reservoirs in South Tahe area of Halahatang oilfield. Tarim Basin. Petrol. Explor. Dev+. 47 (2), 286–296. https://doi.org/10.1016/S1876-3804(20)60048-9.

Dong, Y., Lu, X., Fan, J., Zhuo, Q., 2018. Fracture characteristics and their influence on gas seepage in tight gas reservoirs in the Kelasu Thrust Belt (Kuqa Depression, NW China). At. Energ. 11 (10), 2808. https://doi.org/10.3390/en11102808.

Engelder, T., 1985. Loading paths to joint propagation during a tectonic cycle: an example from the Appalachian Plateau, USA. J. Struct. Geol. 7 (3–4), 459–476. https://doi.org/10.1016/0191-8141(85)90049-5.

Fall, A., Eichhubl, P., Bodnar, R.J., Laubach, S.E., Davis, J.S., 2015. Natural hydraulic fracturing of tight-gas sandstone reservoirs, Piceance Basin, Colorado. GSA Bull 127 (1–2), 61–75. https://doi.org/10.1130/B31021.1.

Fall, A., Ukar, E., Laubach, S.E., 2016. Origin and timing of Dauphiné twins in quartz cement in fractured sandstones from diagenetic environments: insight from fluid inclusions. Tectonophysics 687, 195–209. https://doi.org/10.1016/j.tecto.2016.08.014.

Feng, J., Ren, Q., Xu, K., 2018. Quantitative prediction of fracture distribution using geomechanical method within Kuqa Depression, Tarim Basin, NW China. J. Petrol. Sci. Eng. 162, 22–34. https://doi.org/10.1016/j.petrol.2017.12.006.

Ferrill, D.A., Morris, A.P., McGinnis, R.N., Smart, K.J., Wigginton, S.S., Hill, N.J., 2017. Mechanical stratigraphy and normal faulting. J. Struct. Geol. 94, 275–302. https://doi.org/10.1016/j.jsg.2016.11.010.

Finkbeiner, T., Barton, C.A., Zoback, M.D., 1997. Relationships among in-situ stress, fractures and faults, and fluid flow: monterey Formation, Santa Maria Basin, California. AAPG Bull. 81 (12), 1975–1999. https://doi.org/10.1306/3B05C6FE-172A-11D7-8645000102C1865D.

Forstner, S.R., Laubach, S.E., 2022. Scale-dependent fracture networks. J. Struct. Geol. 165, 104748 https://doi.org/10.1016/j.jsg.2022.104748.

Gale, J.F., Lander, R.H., Reed, R.M., Laubach, S.E., 2010. Modeling fracture porosity evolution in dolostone. J. Struct. Geol. 32 (9), 1201–1211. https://doi.org/10.1016/j.jsg.2009.04.018.

Galuppo, C., Toscani, G., Turrini, C., Bonini, L., Seno, S., 2016. Fracture patterns evolution in sandbox fault-related anticlines. Italian. J. Geosci-Czech. 135, 5–16. https://doi.org/10.3301/IJG.2014.39.

Gan, R., Zhang, H., Chen, J., Huang, W., Zhang, X., Liu, B., Zhang, T., Wang, W., Wei, G., Elekwachi, A., Sultan, G., et al., 2022. Understanding the natural fracture system in the ultra-deep sandstone reservoir using high-definition oil-based microresistivity image logs, case study from Junggar Basin. In: SPE/AAPG/SEG Unconventional Resources Technology Conference, pp. 1–10. https://doi.org/10.15530/urtec-2022-3702216.

Gong, L., Yao, J.Q., Gao, S., Wei, B., Zeng, L.B., Fu, X.F., Gao, Z.Y., Zu, K.W., Tian, H., 2018. Controls of rock mechanical stratigraphy on tectonic fracture spacing. Geotect. Metallogenia 42 (6), 965–973. https://doi.org/10.16539/j.ddgzyckx.2018.06.002.

Gong, L., Gao, M.Z., Zeng, L.B., Fu, X.F., Gao, Z.Y., Gao, A., Zu, K.W., Yao, J.Q., 2017. Controlling factors on fracture development in the tight sandstone reservoirs: a case study of Jurassic-Neogene in the Kuqa foreland basin. Nat. Gas Geosci. 28 (2), 199–208. https://doi.org/10.11764/j.issn.1672-1926.2016.12.003.

Gong, X., Shi, Z., Tian, Y., Zhou, X., Li, W., Wang, Y., 2020. Later fluid alteration of eogenetic karst spaces in carbonate: insights from the Cambrian Longwangmiao Formation, Northwestern Sichuan Basin, China. Carbonate. Evaporite. Carbonates Evaporites 35 (3), 1–18. https://doi.org/10.1007/s13146-020-00606-4.

Gong, L., Zeng, L.B., Du, Y.J., Han, Z.R., 2015. Influences of structural diagenesis on fracture effectiveness: a case study of the Cretaceous tight sandstone reservoirs of Kuqa foreland basin. J. China Univ. Min. Technol. 44 (3), 514–519. https://doi.org/10.13247/j.cnki.jcumt.000263.

Guo, T.L., 2016. Key geological issues and main controls on accumulation and enrichment of Chinese shale gas. Petrol. Explor. Dev+. 43 (3), 349–359. https://doi.org/10.1016/S1876-3804(16)30042-8.

Guo, Y.T., Chen, J.H., Yang, C.H., Mao, H.J., 2012. Distribution characteristics of rock mechanical parameters for deep drilling sections of carbonate rock in Northeast Sichuan. Rock Soil Mech. 33 (1), 161–169. https://doi.org/10.16285/j.rsm.2012.s1.004.

Guo, X., Hu, D., Li, Y., Duan, J., Ji, C., Duan, H., 2018. Discovery and theoretical and technical innovations of Yuanba gas field in Sichuan Basin, SW China. Petrol. Explor. Dev+. 45, 15–28. https://doi.org/10.1016/S1876-3804(18)30002-8.

Guo, X.W., Liu, K.Y., Jia, C.Z., Song, Y., Zhao, M.J., Zhuo, Q.G., Lu, X.S., 2016. Constraining tectonic compression processes by reservoir pressure evolution: overpressure generation and evolution in the Kelasu Thrust Belt of Kuqa Foreland Basin, NW China. Mar. Petrol. Geol. 72, 30–44. https://doi.org/10.1016/j.marpetgeo.2016.01.015.

Han, J.F., Su, Z., Chen, L.X., Guo, D.S., Zhang, Y.T., Ji, Y.Q., Zhang, H.F., Yuan, J.Y., 2019. Reservoir-controlling and accumulation-controlling of strike-slip faults and exploration potential in the platform of Tarim Basin. Acta Petrol. Sin. 40 (11), 1296–1310. https://doi.org/10.7623/syxb201911002.

Han, X., Deng, S., Tang, L., Cao, Z., 2017. Geometry, kinematics and displacement characteristics of strike-slip faults in the northern slope of Tazhong uplift in Tarim Basin: a study based on 3D seismic data. Mar. Petrol. Geol. 88, 410–427. https://doi.org/10.1016/j.marpetgeo.2017.08.033.

Han, J.F., Zhang, H.Z., Yu, H.F., Ji, Y.G., Sun, C.H., Han, J., Dong, R.X., 2012. Hydrocarbon accumulation characteristic and exploration on large marine carbonate condensate field in Tazhong Uplift. Acta Petrol. Sin. 28, 769–782. https://doi.org/10.1007/s11783-011-0280-z.

Hanks, C.L., Lorenz, J., Teufel, L., Krumhardt, A.P., 1997. Lithological and structural controls on natural fracture distribution and behavior within the Lisburne group, northeastern Brooks Range and north slope subsurface, Alaska. AAPG Bull. 81 (10), 1700–1720. https://doi.org/10.1016/S0013-7952(96)00100-7.

Hausegger, S., Kurz, W., Rabitsch, R., Kiechl, E., Brosch, F.J., 2010. Analysis of the internal structure of a carbonate damage zone: implications for the mechanisms of fault breccia formation and fluid flow. J. Struct. Geol. 32 (9), 1349–1362. https://doi.org/10.1016/j.jsg.2009.04.014.

He, Z.L., Jin, X.H., Wo, Y.J., Li, H.L., Bai, Z.R., Jiao, C.L., Zhang, Z.P., 2016. Hydrocarbon accumulation characteristics and exploration domains of ultradeep marine carbonates in China. China. Pet. Explor. 21 (1), 12. https://doi.org/10.3969/j.issn.1672-7703.2016.01.001.

He, J.M., Wang, X.Y., Sun, J.F., Sun, X.T., Shi, J.X., Cao, D.S., Zeng, L.B., 2019. Characteristics and main controlling factors of natural fractures in the Lower-to-Middle Ordovician carbonate reservoirs in Tahe area, Northern Tarim Basin. Oil Gas Geol. 40 (5), 1022–1030. https://doi.org/10.11743/ogg20190507.

Heap, M.J., Baud, P., Reuschlé, T., Meredith, P.G., 2014. Stylolites in limestones: barriers to fluid flow? Geol. 42, 51–54. https://doi.org/10.1130/G34900.1.

Hobbs, D.W., 1967. The formation of tension joints in sedimentary rocks: an explanation. Geol. Mag. 104 (6), 550–556. https://doi.org/10.1017/S0016756800050226.

Hood, S.D., Nelson, C.S., Kamp, P.J., 2004. Burial dolomitisation in a non-tropical carbonate petroleum reservoir: the oligocene tikorangi formation, taranaki basin, New Zealand. Sediment. Geol. 172 (1–2), 117–138. https://doi.org/10.1016/j.sedgeo.2004.08.005.

Hooker, J.N., Gale, J.F.W., Gomez, L.A., Laubach, S.E., Marrett, R., Reed, R., 2009. Aperture-size scaling variations in a low-strain opening-mode fracture set, Cozzette Sandstone, Colorado. J. Struct. Geol. 31 (7), 707–718. https://doi.org/10.1016/j.jsg.2009.04.001.

Huang, C., Yun, L., Cao, Z.C., Lyu, H.T., Li, H.Y., Liu, Y.L., Han, J., 2022. Division and formation mechanism of fault-controlled fracture-vug system of the Middle-to-Lower Ordovician, Shunbei area, Tarim Basin. Oil Gas Geol. 43 (1), 54–68. https://doi.org/10.11743/ogg20220105.

Jamison, W., Pope, A., 1996. Geometry and evolution of a fault-bend fold: mount Bertha Anticline. Geol. Soc. Am. Bull. 108, 208–224. https://doi.org/10.1130/0016-7606(1996)108<0208:GAEOAF>2.3.CO;2.

Jia, C.Z., Ma, D.B., Yuan, J.Y., Wei, G.Q., Yang, M., Yan, L., Tian, F.L., Jiang, L., 2021. Structural characteristics, formation & evolution and genetic mechanisms of strike-slip faults in the Tarim Basin. Nat. Gas. Ind. 41 (8), 81–91. https://doi.org/10.1016/j.ngib.2021.08.017.

Jia, J.K., 2019. Study on Pore-Fluid Pressure of the Ordovician Carbonate Reservoir in Shuntuoguole Low-Uplift, Tarim Basin. PhD Thesis. China University of Petroleum. https://doi.org/10.27643/d.cnki.gsybu.2019.000109.

Kim, Y.S., Peacock, D.C.P., Sanderson, D.J., 2004. Fault damage zones. J. Struct. Geol. 26, 503–517. https://doi.org/10.1016/j.jsg.2003.08.002.

Jia, C.Z., Pang, X.Q., 2015. Research processes and main development directions of deep hydrocarbon geological theories. Acta Petrol. Sin. 36 (12), 1457–1469. https://doi.org/10.7623/syxb201512001.

Kim, Y.S., Peacock, D.C.P., Sanderson, D.J., 2003. Mesoscale strike-slip faults and damage zones at Marsalforn, Gozo Island, Malta. J. Struct. Geol. 25 (5), 793–812. https://doi.org/10.1016/S0191-8141(02)00200-6.

Klimczak, C., Schultz, R.A., Parashar, R., Reeves, D.M., 2010. Cubic law with aperture-length correlation: implications for network scale fluid flow. Hydrogeol. J. 18 (4), 851–862. https://doi.org/10.1007/s10040-009-0572-6.

Krézsek, C., Filipescu, S., Silye, L., Matenco, L., Doust, H., 2010. Miocene facies associations and sedimentary evolution of the Southern Transylvanian Basin (Romania): implications for hydrocarbon exploration. Mar. Petrol. Geol. 27 (1), 191–214. https://doi.org/10.1016/j.marpetgeo.2009.07.009.

Kuchuk, F., Biryukov, D., Fitzpatrick, T., 2015. Fractured-reservoir modeling and interpretation. SPE J. 20, 983–1004. https://doi.org/10.2118/176030-PA.

Lai, J., Chen, K., Xin, Y., Wu, X., Chen, X., Yang, K., Song, Q., Wang, G., Ding, X., 2021. Fracture characterization and detection in the deep Cambrian dolostones in the Tarim Basin, China: insights from borehole image and sonic logs. J. Petrol. Sci. Eng. 196, 107659 https://doi.org/10.1016/j.petrol.2020.107659.

Lai, J., Li, D., Ai, Y., Liu, H., Cai, D., Chen, K., Wang, G., 2022. Structural diagenesis in ultra-deep tight sandstones in the Kuqa depression, Tarim Basin, China. Solid. Earth 13 (6), 975–1002. https://doi.org/10.5194/se-13-975-2022.

Lai, J., Li, D., Bai, T., Zhao, F., Ai, Y., Liu, H., Cai, D., Wang, G., Chen, K., Xie, Y., 2023. Reservoir quality evaluation and prediction in ultra-deep tight sandstones in the Kuqa depression, China. J. Struct. Geol. 170, 104850 https://doi.org/10.1016/j.jsg.2023.104850.

Lan, X., Lü, X., Zhu, Y., Yu, H., 2015. The geometry and origin of strike-slip faults cutting the Tazhong low rise megaanticline (central uplift, Tarim Basin, China) and their control on hydrocarbon distribution in carbonate reservoirs. J. Nat. Gas Sci. Eng. 22, 633–645. https://doi.org/10.1016/j.jngse.2014.12.030.

Lander, R.H., Laubach, S.E., 2015. Insights into rates of fracture growth and sealing from a model for quartz cementation in fractured sandstones. Geol. Soc. Am. Bull. 127, 516–538. https://doi.org/10.1130/B31092.1.

Laubach, S.E., 1997. A method to detect natural fracture strike in sandstones. AAPG Bull. 81 (4), 604–623. https://doi.org/10.1306/522B43E3-1727-11D7-8645000102C1865D.

Laubach, S.E., 2003. Practical approaches to identifying sealed and open fractures. AAPG Bull. 87 (4), 561–579. https://doi.org/10.1306/11060201106.

Laubach, S.E., Eichhubl, P., Hilgers, C., Lander, R.H., 2010. Structural diagenesis. J. Struct. Geol. 32, 1866–1872. https://doi.org/10.1016/j.jsg.2010.10.001, 10.1306/522B43E3-1727-11D7-8645000102C1865D.

Laubach, S.E., Fall, A., Copley, L.K., Marrett, R., Wilkins, S.J., 2016. Fracture porosity creation and persistence in a basement-involved laramide fold, upper cretaceous frontier formation, green river basin, USA. Geol. Mag. 153 (5–6), 887–910. https://doi.org/10.1017/S0016756816000157.

Laubach, S.E., Lander, R.H., Criscenti, L.J., Anovitz, L.M., Urai, J.L., Pollyea, R.M., Hooker, J.N., Narr, W., Evans, M.A., Kerisit, S.N., Olson, J.E., Dewers, T., Fisher, D., Bodnar, R., Evans, B., Dove, P., Bonnell, L.M., Marder, M.P., Pyrak-Nolte, L., 2019. The role of chemistry in fracture pattern development and opportunities to advance interpretations of geological materials. Rev. Geophys. 57, 1065–1111. https://doi.org/10.1029/2019RG000671.

Laubach, S.E., Olson, J.E., Gale, J.F.W., 2004a. Are open fractures necessarily aligned with maximum horizontal stress? Earth Planet Sci. Lett. 222 (1), 191–195. https://doi.org/10.1016/j.epsl.2004.02.019.

Laubach, S.E., Olson, J.E., Gross, M.R., 2009. Mechanical and fracture stratigraphy. AAPG Bull. 93 (11), 1413–1426. https://doi.org/10.1306/07270909094.

Laubach, S.E., Reed, R.M., Olson, J.E., Lander, R.H., Bonnell, L.M., 2004b. Coevolution of crack-seal texture and fracture porosity in sedimentary rocks: cathodoluminescence observations of regional fractures. J. Struct. Geol. 26, 967–982. https://doi.org/10.1016/j.jsg.2003.08.019.

Laubach, S.E., Ward, M.E., 2006. Diagenesis in porosity evolution of opening-mode fractures, middle triassic to lower jurassic La boca formation, NE Mexico. Tectonophysics 419 (1–4), 75–97. https://doi.org/10.1016/j.tecto.2006.03.020.

Laubach, S.E., Zeng, L., Hooker, J.N., Wang, Q., Zhang, R., Wang, J., Ren, B., 2023. Deep and ultra-deep basin brittle deformation with focus on China. J. Struct. Geol. 175, 104938 https://doi.org/10.1016/j.jsg.2023.104938.

Lavoie, D., Chi, G., 2001. The Lower Silurian Sayabec Formation in northern Gaspé: carbonate diagenesis and reservoir potential. Bull. Can. Petrol. Geol. 49 (2), 282–298. https://doi.org/10.2113/49.2.282.

Li, H., Lin, C., Ren, L., Zhang, G., Chang, L., Dong, C., 2021a. Quantitative prediction of multi-period tectonic fractures based on integrated geological-geophysical and geomechanics data in deep carbonate reservoirs of Halahatang oilfield in northern Tarim Basin. Mar. Petrol. Geol. 134, 105377 https://doi.org/10.1016/j.marpetgeo.2021.105377.

Li, J.Z., Tao, X.W., Bai, B., Huang, S.P., Jiang, Q.C., Zhao, Z.Y., Chen, Y.Y., Ma, D.B., Zhang, L.P., Li, N.X., Song, W., 2021b. Geological conditions, reservoir evolution and favorable exploration directions of marine ultra-deep oil and gas in China. Petrol. Explor. Dev. 48 (1), 52–67. https://doi.org/10.1016/S1876-3804(21)60005-8.

Li, L., Tang, H.M., Wang, X., Liao, J.J., Qi, B.L., Zhao, F., Zhang, L.H., Feng, W., Tang, H.X., Shi, L., 2018a. Evolution of diagenetic fluid of ultra-deep cretaceous Bashijiqike Formation in Kuqa depression. J. Cent. South. Univ. 25 (10), 2472–2495. https://doi.org/10.1007/s11771-018-3930-5.

Li, Y., Hou, G., Hari, K.R., Neng, Y., Lei, G., Tang, Y., Zhou, L., Sun, S., Zheng, C., 2018b. The model of fracture development in the faulted folds: the role of folding and faulting. Mar. Petrol. Geol. 89, 243–251. https://doi.org/10.1016/j.marpetgeo.2017.05.025.

Li, Z., Luo, W., Zeng, B.Y., Liu, J.Q., Yu, J.B., 2018c. Fluid-rock interactions and reservoir formation driven by multiscale structural deformation in basin evolution. Earth Sci. 43 (10), 3498–3510. https://doi.org/10.3799/dqkx.2018.323.

Liu, G.P., Zeng, L.B., Han, C.Y., Mehdi, O., Lyu, W.Y., Wang, Q.Q., Zhu, J.W., Hou, F.X., 2020. Natural fractures in carbonate basement reservoirs of the Jizhong Sub-Basin, Bohai Bay Basin, China: key aspects favoring oil production. Energies 13 (18), 4635. https://doi.org/10.3390/en13184635.

Li, Y., Xu, S., 2017. Reservoir fracture cave characteristics of middle - lower Ordovician carbonate rocks in Tahe oilfield in Tarim Basin, China. Indian J. Mar. Sci. 46, 2191–2200. https://doi.org/10.4156/aiss.vol5.issue6.140.

Liu, G.P., Zeng, L.B., Zhu, R., Gong, L., Ostadhassan, M., Mao, Z., 2021. Effective fractures and their contribution to the reservoirs in deep tight sandstones in the Kuqa Depression, Tarim Basin, China. Mar. Petrol. Geol. 124, 104824 https://doi.org/10.1016/j.marpetgeo.2020.104824.

Liu, J.S., Ding, W.L., Yang, H.M., Dai, P., Wu, Z.H., Zhang, G.J., 2022. Natural fractures and rock mechanical stratigraphy evaluation in the Huaqing area, Ordos Basin: a quantitative analysis based on numerical simulation. Earth Sci. 1–19. https://kns.cnki.net/kcms/detail/42.1874.P.20220711.0942.004.html.

Liu, J., Liu, G., 2017. Types, evolution of fractures, and their relationship with oil and gas migration of permian changxing formation in yuanba gas field of Sichuan Basin. China. Energ. Fuel. 31, 9345–9355. https://doi.org/10.1021/acs.energyfuels.7b01893.

Liu, J., Polak, A., Elsworth, D., Grader, A., 2005. Dissolution-induced preferential flow in a limestone fracture. J. Contam. Hydrol. 78 (1–2), 53–70. https://doi.org/10.1016/j.jconhyd.2005.03.001.

Liu, B.Z., 2020. Analysis of main controlling factors of oil and gas differential accumulation in Shunbei area, Tarim Basin-taking Shunbei No.1 and No.5 strike slip fault zones as examples. China Pet. Explor 25 (3), 83–95. CNKI:SUN:KTSY.0.2020-03-008.

Liu, Q., Zhu, D., Jin, Z., Liu, C., Zhang, D., He, Z., 2016. Coupled alteration of hydrothermal fluids and thermal sulfate reduction (TSR) in ancient dolomite reservoirs – an example from Sinian Dengying Formation in Sichuan Basin, southern China. Precambrian Res. 285, 39–57. https://doi.org/10.1016/j.precamres.2016.09.006.

Lyu, Y., Ma, H., Wang, Z., Deng, G., Wen, H., 2022. Genetic Types of the tp12cx Strike-Slip Fault segments and their role in controlling reservoirs in the Tarim Basin. Front. Earth. 10, 916475 https://doi.org/10.3389/feart.2022.916475.

Ma, D.B., Wu, G.H., Scarselli, N., Luo, X.S., Han, J.F., Chen, Z.Y., 2019. Seismic damage zone and width–throw scaling along the strike-slip faults in the Ordovician carbonates in the Tarim Basin. Petrol. Sci. 16, 752–762. https://doi.org/10.1007/s12182-019-0352-4.

Ma, X., Wang, H., Zhou, S., Shi, Z., Zhang, L., 2021. Deep shale gas in China: geological characteristics and development strategies. Energy Rep. 7, 1903–1914. https://doi.org/10.1016/j.egyr.2021.03.043.

Ma, Y.S., Cai, X.Y., Yun, L., Li, Z., Li, H., Deng, S., Zhao, P., 2022. Practice and theoretical and technical progress in exploration and development of Shunbei ultra-deep carbonate oil and gas field, Tarim Basin, NW China. Petrol. Explor. Dev. 49, 1–20. https://doi.org/10.1016/S1876-3804(22)60001-6.

Ma, Y.S., Cai, X.Y., Zhao, P.R., Zhang, X.F., 2010. Formation mechanism of deep-buried carbonate reservoir and its model of three-element controlling reservoir: a case study from the Puguang Oilfield in Sichuan. Acta Geol. Sin. 84 (8), 1087–1094. CNKI:SUN:DZXE.0.2010-08-002.

Ma, Y.S., Guo, T.L., Zhao, X.F., Cai, X.Y., 2007. Formation mechanism of deep high-quality dolomite reservoir in Puguang gas field. Sci. China Earth Sci. 37, 43–52. https://doi.org/10.1007/s11430-008-5008-y.

Mao, C., Zhong, J., Li, Y., Wang, Y., Niu, Y., Ni, L., Shao, Z., 2014. Ordovician carbonate rock matrix fractured-porous reservoirs in Tahe Oilfield, Tarim Basin, NW China. Petrol. Explor. Dev+. 41, 745–753. https://doi.org/10.1016/S1876-3804(14)60088-4.

Mao, Z., Zeng, L.B., Liu, G.D., Liu, G.P., Tian, H., Dong, S., Lyu, W.Y., Ostadhassan, M., 2022. Controls of fault-bend fold on natural fractures: insight from discrete element simulation and outcrops in the southern margin of the Junggar Basin, Western China. Mar. Petrol. Geol. 138, 105541 https://doi.org/10.1016/j.marpetgeo.2022.105541.

Mao, Z., Zeng, L.B., Liu, G.P., Gao, Z.Y., Tian, H., Liao, Q., Zhang, Y.Z., 2020. Characterization and effectiveness of natural fractures in deep tight sandstones at the south margin of the Junggar Basin, northwestern China. Oil Gas Geol. 41 (6), 1212–1221. https://doi.org/10.11743/ogg20200609.

McDermott, C.I., Edlmann, K., Haszeldine, R.S., 2013. Predicting hydraulic tensile fracture spacing in strata-bound systems. Int. J. Rock. Mech. Min. 63, 39–49. https://doi.org/10.1016/j.ijrmms.2013.06.004.

McGrath, A.G., Davison, I., 1995. Damage zone geometry around fault tips. J. Struct. Geol. 17 (7), 1011–1024. https://doi.org/10.1016/0191-8141(94)00116-H.

Mejia, C., Roehl, D., Rueda, J., Fonseca, F., 2022. Geomechanical effects of natural fractures on fluid flow in a pre-salt field. J. Nat. Gas Sci. Eng. 107, 104772 https://doi.org/10.1016/j.jngse.2022.104772.

Méndez, J.N., Jin, Q., González, M., Zhang, X., Lobo, C., Boateng, C.D., Zambrano, M., 2020. Fracture characterization and modeling of karsted carbonate reservoirs: a case study in Tahe oilfield, Tarim Basin (western China). Mar. Petrol. Geol. 112, 104104 https://doi.org/10.1016/j.marpetgeo.2019.104104.

Meng, Q.F., Hao, F., Tian, J.Q., 2021. Origins of non-tectonic fractures in shale. Earth Sci. Rev. 222, 103825 https://doi.org/10.1016/j.earscirev.2021.103825.

Meng, Q.F., Hooker, J., Cartwright, J., 2017. Genesis of natural hydraulic fractures as an indicator of basin inversion. J. Struct. Geol. 102, 1–20. https://doi.org/10.1016/j.jsg.2017.07.001.

Micarelli, L., Moretti, I., Jaubert, M., Moulouel, H., 2006. Fracture analysis in the south-western Corinth rift (Greece) and implications on fault hydraulic behavior. Tectonophysics 426 (1–2), 31–59. https://doi.org/10.1016/j.tecto.2006.02.022.

Miller, R.B., 1994. A mid-crustal contractional stepover zone in a major strike-slip system, North Cascades, Washington. J. Struct. Geol. 16 (1), 47–60. https://doi.org/10.1016/0191-8141(94)90017-5.

Mitchell, T.M., Faulkner, D.R., 2009. The nature and origin of off-fault damage surrounding strike-slip fault zones with a wide range of displacements: a field study from the Atacama fault system, northern Chile. J. Struct. Geol. 31 (8), 802–816. https://doi.org/10.1016/j.jsg.2009.05.002.

Mourgues, R., Bureau, D., Bodet, L., Gay, A., Gressier, J.B., 2012. Formation of conical fractures in sedimentary basins: experiments involving pore fluids and implications for sandstone intrusion mechanisms. Earth Planet Sci. Lett. 313, 67–78. https://doi.org/10.1016/j.epsl.2011.10.029.

Narr, W., 1991. Fracture density in the deep subsurface: techniques with application to point Arguello oil field. AAPG Bull. 75 (8), 1300–1323. https://doi.org/10.1306/0C9B2939-1710-11D7-8645000102C1865D.

Narr, W., Suppe, J., 1991. Joint spacing in sedimentary rocks. J. Struct. Geol. 13 (9), 1037–1048. https://doi.org/10.1016/0191-8141(91)90055-N.

Nelson, R.A., 2001. Geologic Analysis of Naturally Fractured Reservoirs. Gulf Professional, Houston.

Neng, Y., Yand, H., Deng, X., 2018. Structural patterns of fault damage zones in carbonate rocks and their influences on petroleum accumulation in Tazhong Paleo-uplift, Tarim Basin, NW China. Petrol. Explor. Dev. 45, 43–54. https://doi.org/10.1016/S1876-3804(18)30004-1.

Ni, J., 1978. Contemporary tectonics in the Tien Shan region. Earth Planet Sci. Lett. 41 (3), 347–354. https://doi.org/10.1016/0012-821X(78)90189-9.

Nian, T., Li, Y., Hou, T., Tan, C., Liu, C., 2020. Natural fractures at depth in the Lower Cretaceous Kuqa Depression tight sandstones: identification and characteristics. Geol. Mag. 157 (8), 1299–1315. https://doi.org/10.1017/S0016756819001444.

Nollet, S., Hilgers, C., Urai, J., 2005. Sealing of fluid pathways in overpressure cells: a case study from the Buntsandstein in the Lower Saxony Basin (NW Germany). Int. J. Earth Sci. 94, 1039–1055. https://doi.org/10.1007/s00531-005-0492-1.

Odling, N.E., 1992. Network properties of a two-dimensional natural fracture pattern. Pure. Appl. Geophys. 138 (1), 95–114. https://doi.org/10.1007/BF00876716.

Odling, N.E., Harris, S.D., Knipe, R.J., 2004. Permeability s caling properties of fault damage zones in siliclastic rocks. J. Struct. Geol. 26 (9), 1727–1747. https://doi.org/10.1016/j.jsg.2004.02.005.

Odling, N.E., Webman, I., 1991. A “conductance” mesh approach to the permeability of natural and simulated fracture patterns. Water Resour. Res. 27 (10), 2633–2643. https://doi.org/10.1029/91WR01382.

Ogata, K., Senger, K., Braathen, A., Tveranger, J., 2014. Fracture corridors as seal-bypass systems in siliciclastic reservoir-cap rock successions: field-based insights from the Jurassic Entrada Formation (SE Utah, USA). J. Struct. Geol. 66, 162–187. https://doi.org/10.1016/j.jsg.2014.05.005.

Olson, J.E., Laubach, S.E., Lander, R.L., 2007. Combining diagenesis and mechanics to quantify fracture aperture distributions and fracture pattern permeability. In: Lonergan, L., Jolley, R.J., Sanderson, D.J., Rawnsley, K. (Eds.), Fractured Reservoirs, 270. Geological Society of London Special Publication, pp. 97–112. https://doi.org/10.1144/GSL.SP.2007.270.01.08.

Peacock, D.C.P., 1991. Displacements and segment linkage in strike-slip fault zones. J. Struct. Geol. 13 (9), 1025–1035. https://doi.org/10.1016/0191-8141(91)90054-M.

Peacock, D.C.P., Sanderson, D.J., 1994. Geometry and development of relay ramps in normal fault systems. AAPG Bbull 78 (2), 147–165. https://doi.org/10.1306/BDFF9046-1718-11D7-8645000102C1865D.

Peng, H., Yin, C., He, Q., Xia, G., Liu, Y., Ma, T., Chen, K., Liu, R., Su, W., 2022. Development characteristics and petroleum geological significance of Permian pyroclastic flow volcanic rocks in Western Sichuan Basin, SW China. Petrol. Explor. Dev+. 49, 64–77. https://doi.org/10.1016/S1876-3804(22)60005-3.

Perez, R.J., Boles, J.R., 2005. Interpreting fracture development from diagenetic mineralogy and thermoelastic contraction modeling. Tectonophysics 400 (1–4), 179–207. https://doi.org/10.1016/j.tecto.2005.03.002.

Philip, Z.G., Jennings Jr., J.W., Olson, J.E., Laubach, S.E., Holder, J., 2005. Modeling coupled fracture-matrix fluid flow in geomechanically simulated fracture networks. SPE Reservoir Eval. Eng. 8 (4), 300–309. https://doi.org/10.2118/77340-PA.

Qi, L.X., 2021. Structural characteristics and storage control function of the shun I fault zone in the Shunbei region, Tarim Basin. J. Petrol. Sci. Eng. 203, 108653 https://doi.org/10.1016/j.petrol.2021.108653.

Qiu, H., Deng, S., Zhang, J., Lin, H., Huang, C., Han, J., Lin, W., Zhu, X., 2022. The evolution of a strike-slip fault network in the Guchengxu High, Tarim Basin (NW China). Mar. Petrol. Geol. 140, 105655 https://doi.org/10.1016/j.marpetgeo.2022.105655.

Railsback, L.B., Andrews, L.M., 1995. Tectonic stylolites in the ‘undeformed’ Cumberland Plateau of southern Tennessee. J. Struct. Geol. 17 (6), 911–915. https://doi.org/10.1016/0191-8141(94)00127-L.

Ravier, E., Guiraud, M., Guillien, A., Vennin, E., Buoncristiani, J.F., Portier, E., 2015. Micro- to macro-scale internal structures, diagenesis and petrophysical evolution of injectite networks in the Vocontian Basin (France): implications for fluid flow. Mar. Petrol. Geol. 64, 125–151. https://doi.org/10.1016/j.marpetgeo.2015.02.040.

Ren, Q., Feng, J., Johnston, S., Peddle, C., Du, H., 2020. Quantitative characterization of interlayer fractures in carbonate rocks based on finite element numerical simulation. J. Petrol. Sci. Eng. 195, 107942 https://doi.org/10.1016/j.petrol.2020.107942.

Rizza, M., Abdrakhmatov, K., Walker, R., Braucher, R., Guillou, V., Carr, A.S., Campbell, G., Mckenzie, D., Jackson, J., Aumaître, G., Bourlès, D.L., Keddadouche, K., 2019. Rate of slip from multiple quaternary dating methods and paleoseismic investigations along the talas-fergana fault: tectonic implications for the tien Shan range. Tectonics 38 (7), 2477–2505. https://doi.org/10.1029/2018TC005188.

Rustichelli, A., Agosta, F., Tondi, E., Spina, V., 2013. Spacing and distribution of bed-perpendicular joints throughout layered, shallow-marine carbonates (Granada Basin, southern Spain). Tectonophysics 582, 188–204. https://doi.org/10.1016/j.tecto.2012.10.007.

Rustichelli, A., Tondi, E., Agosta, F., Cilona, A., Giorgioni, M., 2012. Development and distribution of bed-parallel compaction bands and pressure solution seams in

carbonates (Bolognano Formation, Majella Mountain, Italy). J. Struct. Geol. 37, 181–199. https://doi.org/10.1016/j.jsg.2012.01.007.
Salvini, F., Storti, F., 2001. The distribution of deformation in parallel fault-related folds with migrating axial surfaces: comparison between fault-propagation and fault-bend folding. J. Struct. Geol. 23 (1), 25–32. https://doi.org/10.1016/S0191-8141(00)00081-X.
Sanderson, D.J., Nixon, C.W., 2015. The use of topology in fracture network characterization. J. Struct. Geol. 72, 55–66. https://doi.org/10.1016/j.jsg.2015.01.005.
Shi, J.X., Zhao, X.Y., Pan, R.F., Zeng, L.B., Luo, W.J., 2022. Natural fractures in the deep Sinian carbonates of the central Sichuan Basin, China: implications for reservoir quality. J. Petrol. Sci. Eng. 216, 110829 https://doi.org/10.1016/j.petrol.2022.110829.
Smart, K.J., Ferrill, D.A., Morris, A.P., 2009. Impact of interlayer slip on fracture prediction from geomechanical models of fault-related folds. AAPG Bull. 93 (11), 1447–1458. https://doi.org/10.1306/05110909034.
Smart, B.G.D., Somerville, J.M., Edlman, K., Jones, C., 2001. Stress sensitivity of fractured reservoirs. J. Petrol. Sci. Eng. 29 (1), 29–37. https://doi.org/10.1016/S0920-4105(00)00088-7.
Su, J., Wang, X., Yang, H., Yu, F., Li, Y., Ma, S., Wei, C., Weng, N., Yang, Y., 2021. Hydrothermal alteration and hydrocarbon accumulations in ultra-deep carbonate reservoirs along a strike-slip fault system, Tarim Basin, NW China. J. Petrol. Sci. Eng. 203, 108605 https://doi.org/10.1016/j.petrol.2021.108605.
Sun, L.D., Zou, C.N., Zhu, R.K., Zhang, Y.H., Zhang, S.C., Zhang, B.M., Zhu, G.Y., Gao, Z. Y., 2013. Formation, distribution and potential of deep hydrocarbon resources in China. Petrol. Explor. Dev+. 40 (6), 641–649. https://doi.org/10.1016/S1876-3804(13)60093-2.
Sun, S., Hou, G., Zheng, C., 2017. Fracture zones constrained by neutral surfaces in a fault-related fold: insights from the Kelasu tectonic zone, Kuqa Depression. J. Struct. Geol. 104, 112–124. https://doi.org/10.1016/j.jsg.2017.10.005.
Suppe, J., 1983. Geometry and kinematics of fault-bend folding. Am. J. Sci. 283 (7), 684–721. https://doi.org/10.2475/ajs.283.7.684.
Suppe, J., Medwedeff, D.A., 1990. Geometry and kinematics of fault-propagation folding. Eclogae Geol. Helv. 83 (3), 409–454. https://doi.org/10.1111/j.1365-3091.1990.tb01987.x.
Tamara, J., Mora, A., Robles, W., Kammer, A., Ortiz, A., Sanchez-Villar, N., Piraquive, A., Rueda, L.H., Casallas, W., Castellanos, J., Montaña, J., Parra, L.G., Corredor, J., Ramirez, Á., Zambrano, E., 2015. Fractured reservoirs in the Eastern Foothills, Colombia, and their relationship with fold kinematics. AAPG Bull. 99, 1599–1633. https://doi.org/10.1306/09291411109.
Tanner, P.W., 1989. The flexural-slip mechanism. J. Struct. Geol. 11 (6), 635–655. https://doi.org/10.1016/0191-8141(89)90001-1.
Tavani, S., Mencos, J., Bausà, J., Muñoz, J.A., 2011. The fracture pattern of the Sant Corneli Bóixols oblique inversion anticline (Spanish Pyrenees). J. Struct. Geol. 33 (11), 1662–1680. https://doi.org/10.1016/j.jsg.2011.08.007.
Tavani, S., Storti, F., Salvini, F., Toscano, C., 2008. Stratigraphic versus structural control on the deformation pattern associated with the evolution of the Mt. Catria anticline. Italy. J. Struct. Geol. 30 (5), 664–681. https://doi.org/10.1016/j.jsg.2008.01.011.
Thompson, J.A., Burbank, D.W., Li, T., Chen, J., Bookhagen, B., 2015. Late Miocene northward propagation of the northeast Pamir thrust system, northwest China. Tectonics 34 (3), 510–534. https://doi.org/10.1002/2014TC003690.
Tian, F., Di, Q., Jin, Q., Cheng, F., Zhang, W., Lin, L., Wang, Y., Yang, D., Niu, C., Li, Y., 2019. Multiscale geological-geophysical characterization of the epigenic origin and deeply buried paleokarst system in Tahe Oilfield, Tarim Basin. Mar. Petrol. Geol. 102, 16–32. https://doi.org/10.1016/j.marpetgeo.2018.12.029.
Tondi, E., Antonellini, M., Aydin, A., Marchegiani, L., Cello, G., 2006. The role of deformation bands, stylolites and sheared stylolites in fault development in carbonate grainstones of Majella Mountain. Italy. J. Struct. Geol. 28 (3), 376–391. https://doi.org/10.1016/j.jsg.2005.12.001.
Ukar, E., Baqués, V., Laubach, S.E., Marrett, R., 2020. The nature and origins of decametre-scale porosity in Ordovician carbonate rocks, Halahatang oilfield, Tarim basin, China. J. Geol. Soc. London. 177, 1074–1091. https://doi.org/10.1144/jgs2019-156.
Ukar, E., Laubach, S.E., 2016. Syn- and postkinematic cement textures in fractured carbonate rocks: insights from advanced cathodoluminescence imaging. Tectonophysics 690, 190–205. https://doi.org/10.1016/j.tecto.2016.05.001.
Ukar, E., Laubach, S.E., Hooker, J.N., 2019. Outcrops as guides to subsurface natural fractures: example from the Nikanassin Formation tight-gas sandstone, Grande Cache, Alberta foothills, Canada. Mar. Petrol. Geol. 103, 255–275. https://doi.org/10.1016/j.marpetgeo.2019.01.039.
Ukar, E., Lopez, R.G., Laubach, S.E., Gale, J.F.W., Manceda, R., Marrett, R., 2017. Microfractures in bed-parallel veins (beef) as predictors of vertical macrofractures in shale: vaca Muerta Formation, Agrio Fold-and-Thrust Belt, Argentina. J. S. Am. Earth. Sci. 79, 152–169. https://doi.org/10.1016/j.jsames.2017.07.015.
Wang, B., Yang, Y., Cao, Z.C., He, S., Zhao, Y.Q., Guo, X.W., Liu, Y.L., Chen, J.X., Zhao, J. X., 2021a. U-Pb dating of calcite veins developed in the Middle-Lower Ordovician reservoirs in Tahe Oilfield and its petroleum geologic significance in Tahe Oilfield. Earth Sci. 46 (9), 3203–3216. https://doi.org/10.3799/dqkx.2020.352.
Wang, J., Wang, H., Zhang, R., Dong, L., Wang, K., Zhang, Z., 2023a. Improvement of reservoir quality of ultra-deep tight sandstones by tectonism and fluid: a case study of Keshen gas field in Tarim Basin, western China. Pet 9 (1), 124–134. https://doi.org/10.1016/j.petlm.2023.01.002.
Wang, J., Yang, X., Zhang, J., Wang, K., Zhang, R., Wang, Q., Ren, B., Ukar, E., 2023b. Subsurface fracture characterization in a folded ultra-deep tight-gas sandstone reservoir: a case study from the Keshen gas field, Tarim Basin, China. J. Struct. Geol. 172, 104867 https://doi.org/10.1016/j.jsg.2023.104867.
Wang, J., Zeng, L., Yang, X., Liu, C., Wang, K., Zhang, R., Chen, X., Qu, Y., Laubach, S.E., Wang, Q., 2021b. Fold-Related fracture distribution in neogene, triassic, and jurassic sandstone outcrops, northern margin of the Tarim Basin, China: guides to deformation in ultradeep tight sandstone reservoirs. Lithosphere-us 2021 (1), 8330561. https://doi.org/10.2113/2021/8330561.
Wang, Q.H., Yang, H.J., Wang, R.J., Li, S.Y., Deng, X.L., Li, C., Chang, L.J., Wan, X.G., Zhang, Y.T., 2021c. Discovery and exploration technology of fault-controlled large oil and gas fields of ultra-deep formation in strike slip fault zone in Tarim Basin. China Pet. Explor. 26 (4), 58–71. https://doi.org/10.3969/j.issn.1672-7703.2021.04.005.
Wang, Y., Zhang, S.N., Liu, Y.L., 2022a. Controls of strike-slip fault activities on hydrocarbon accumulation in Tahe Oilfield, Tarim Basin. Pet. Geol. Exp. 44 (3), 394–401. https://doi.org/10.11781/sysydz202203394.
Wang, Y.F., Zhao, X.Y., Liu, C.C., 2019a. Development characteristics and main controlling factors of natural fractures in reef-flat facies reservoirs of Changxing Formation in Yuanba area, northeastern Sichuan Basin. Nat. Gas Geosci. 30 (7), 973–981. https://doi.org/10.11764/j.issn.1672-1926.2019.04.004.
Wang, Z., Lyu, X., Wang, S., Li, Y., Zhou, X., Quan, H., Li, R., 2020a. Fracture systems and petrophysical properties of tight sandstone undergoing regional folding: a case study of the Cretaceous reservoirs in the Kuqa foreland thrust belt. Tarim Basin. Mar. Petrol. Geol. 112, 104055 https://doi.org/10.1016/j.marpetgeo.2019.104055.
Wang, Z., Gao, Z., Fan, T., Zhang, H., Qi, L., Yun, L., 2019b. Hydrocarbon-bearing characteristics of the SB1 strike-slip fault zone in the north of the shuntuo low uplift, tarim basin. Petrol. Geosci. 27 (1), 1–15. https://doi.org/10.1144/petgeo2019-144.
Wang, Z., Gao, Z., Fan, T., Zhang, H., Yuan, Y., Wei, D., Qi, L., Yun, L., Karubandika, G. M., 2022b. Architecture of strike-slip fault zones in the central Tarim Basin and implications for their control on petroleum systems. J. Petrol. Sci. Eng. 213, 110432 https://doi.org/10.1016/j.petrol.2022.110432.
Wang, Z., Lyu, X., Li, Y., Liang, H., Li, L., He, T., 2021d. Natural fracture opening preservation and reactivation in deep sandstones of the Kuqa foreland thrust belt. Tarim Basin. Mar. Petrol. Geol. 127, 104956 https://doi.org/10.1016/j.marpetgeo.2021.104956.
Wang, Z.M., Xie, H.W., Li, Y., Lei, G.L., Wu, C., Yang, X.Z., Ma, Y.J., Neng, Y., 2013. Exploration and discovery of large and deep subsalt gas fields in Kuqa foreland thrust belt. China. Pet. Explor. 18 (3), 1–11. https://doi.org/10.3969/j.issn.1672-7703.2013.03.001.
Wang, Z.Y., Gao, Z., Fan, T., Shang, Y., Qi, L., Yun, L., 2020b. Structural characterization and hydrocarbon prediction for the SB5M strike-slip fault zone in the Shuntuo Low Uplift, Tarim Basin. Mar. Petrol. Geol. 117, 104418 https://doi.org/10.1016/j.marpetgeo.2020.104418.
Wardlaw, N.C., Cassan, J.P., 1978. Estimation of recovery efficiency by visual observation of pore systems in reservoir rocks. Bull. Can. Petrol. Geol. 26 (4), 572–585. https://doi.org/10.35767/gscpgbull.26.4.572.
Watkins, H., Butler, R.W.H., Bond, C.E., Healy, D., 2015. Influence of structural position on fracture networks in the Torridon Group, Achnashellach fold and thrust belt, NW Scotland. J. Struct. Geol. 74, 64–80. https://doi.org/10.1016/j.jsg.2015.03.001.
Wei, G., Zhang, R., Yu, C., Zhang, K., Wang, K., 2023. Coupled relationships between sandstone overburden stress and ultra-deep reservoir brittle deformation properties based on in situ CT scanning. J. Struct. Geol. 173, 104905. https://doi.org/10.1016/j.jsg.2023.104905.
Weisenberger, T., Eichhubl, P., Laubach, S.E., Fall, A., 2019. Degradation of fracture porosity by carbonate cement, Piceance basin, Colorado, USA. Petrol. Geosci. 25, 354–370. https://doi.org/10.1144/petgeo2018-162.
Wen, L., Wang, H., Xu, L., Zhang, Y., Yuan, H.F., Chen, S.L., Qiao, Y.P., Chen, C., 2021. Characteristics and main controlling factors of gas accumulation of the middle permian qixia formation in western Sichuan Basin. China Pet. Explor. 26 (6), 68–81. https://doi.org/10.3969/j.issn.1672-7703.2021.06.005.
Wennberg, O.P., Casini, G., Jonoud, S., Peacock, D.C.P., 2016. The characteristics of open fractures in carbonate reservoirs and their impact on fluid flow: a discussion. Petrol. Geosci. 22, 91–104. https://doi.org/10.1144/petgeo2015-003.
Westaway, R., 1995. Deformation around stepovers in strike-slip fault zones. J. Struct. Geol. 17 (6), 831–846. https://doi.org/10.1016/0191-8141(94)00098-K.
Wu, G., Ma, B., Han, J., Guan, B., Chen, X., Yang, P., Xie, Z., 2021. Origin and growth mechanisms of strike-slip faults in the central Tarim cratonic basin, NW China. Petrol. Explor. Dev+. 48, 595–607. https://doi.org/10.1016/S1876-3804(21)60048-4.
Wu, G., Xie, E., Zhang, Y., Qing, H., Luo, X., Sun, C., 2019. Structural diagenesis in carbonate rocks as identified in fault damage zones in the northern Tarim Basin, NW China. Minerals-Basel 9 (6), 360. https://doi.org/10.3390/min9060360.
Wu, J., Fan, T., Gao, Z., Yin, X., Fan, X., Li, Chen chen, Yu, W., Li, Chen, Zhang, C., Zhang, J., Sun, X., 2018. A conceptual model to investigate the impact of diagenesis and residual bitumen on the characteristics of Ordovician carbonate cap rock from Tarim Basin, China. J. Petrol. Sci. Eng. 168, 226–245. https://doi.org/10.1016/j.petrol.2018.05.034.
Wu, J., Wang, Q., Cheng, X., Cheng, F., Yu, X., Zhang, C., Shen, X., Guo, Z., 2023. Formation of multi-stage and clustered fractures at 3.6 to 4.9 km in the shizigou structure, SW qaidam basin. J. Struct. Geol. 169, 104845 https://doi.org/10.1016/j.jsg.2023.104845.
Xu, K., Zhang, H., Ju, W., Yin, G.Q., Wang, H.M., Wang, Z.M., Wang, C.H., Li, C., Yuan, F., Zhao, W., 2022. Effective fracture distribution and its influence on natural gas productivity of ultra-deep reservoir in Bozi-X block of Kuqa depression. Earth Sci. 1–26. https://kns.cnki.net/kcms/detail/42.1874.P.20220713.1806.002.html.
Xu, X.H., Chen, Q.L., Chu, C.L., Li, G.R., Liu, C.G., Shi, Z., 2017. Tectonic evolution and paleokarstification of carbonate rocks in the Paleozoic Tarim Basin. Carbonate. Evaporite. Carbonates and Evaporites 32 (4), 487–496. https://doi.org/10.1007/s13146-016-0307-4.

Yang, H.F., 2015. Recent advances in imaging crustal fault zones: a review. Earthq. Sci. 28 (2), 151–162. https://doi.org/10.1007/s11589-015-0114-3.
Yang, H.J., Shen, J.W., Wang, X., Zhang, L.J., Li, M., 2011. Controls on reservoir quality in the paleogene Kalatar Formation of the southwestern region of the Tarim Basin, China. Petrol. Sci. 8 (3), 302–315. https://doi.org/10.1007/s12182-011-0147-8.
Yang, R., Ding, W., Liu, J., Zhao, Z., Li, S., Xiao, Z., 2020. Fracture identification of Ordovician carbonate reservoir based on R/S analysis in the north of Shunbei No.5 fault zone, Tarim Basin. Interpret 8, 907–916. https://doi.org/10.1190/int-2019-0284.1.
Yang, X.W., Tian, J., Wang, Q.H., Li, Y.L., Yang, H.J., Li, Y., Tang, Y.G., Yuan, W.F., Huang, S.Y., 2021. Geological understanding and favorable exploration fields of ultra-deep formations in Tarim Basin. China Pet. Explor. 26 (4), 17–28. https://doi.org/10.3969/j.issn.1672-7703.2021.04.002.
Ye, N., Li, Y., Huang, B., Xi, B., Jiang, H., Lu, Z., Chen, Q., You, D., Xu, J., 2022. Hydrothermal silicification and its impact on lower–middle ordovician carbonates in shunnan area, Tarim Basin, NW China. Geol. J. 57, 3538–3557. https://doi.org/10.1002/gj.4482.
Yu, J., Shi, K., Wang, Q., Liu, B., Han, J., Song, Y., Kong, Y., Jiang, W., 2022. Structural diagenesis of deep carbonate rocks controlled by intra-cratonic strike-slip faulting: an example in the Shunbei area of the Tarim Basin, NW China. Basin Res. 34 (5), 1601–1631. https://doi.org/10.1111/bre.12672.
Yun, L., 2021. Controlling effect of NE strike-slip fault system on reservoir development and hydrocarbon accumulation in the eastern Shunbei area and its geological significance, Tarim Basin. China Pet. Explor. 26 (3), 41–52. https://doi.org/10.3969/j.issn.1672-7703.2021.03.004.
Zeng, L.B., 2010. Microfracturing in the upper triassic Sichuan Basin tight-gas sandstones: tectonic, overpressure, and diagenetic origins. AAPG Bull. 94, 1811–1825. https://doi.org/10.1306/06301009191.
Zeng, L.B., Li, X.Y., 2009. Fractures in sandstone reservoirs with ultra-low permeability: a case study of the upper triassic yanchang formation in the Ordos basin, China. AAPG Bull. 93, 461–477. https://doi.org/10.1306/09240808047.
Zeng, L.B., Lyu, P., Qu, X.F., Fan, J.M., 2020. Multi-scale fractures in tight sandstone reservoirs with low permeability and geological conditions of their development. Oil Gas Geol. 41 (3), 449–454. CNKI:SUN:SYYT.0.2020-03-002.
Zeng, L.B., Lyu, W., Li, J., Zhu, L., Weng, J., Yue, F., Zu, K., 2016. Natural fractures and their influence on shale gas enrichment in Sichuan Basin, China. J. Nat. Gas Sci. Eng. 30, 1–9. https://doi.org/10.1016/j.jngse.2015.11.048.
Zeng, L.B., Qi, J.F., Wang, Y.X., 2007. The origin type of tectonic fractures and its geological formation conditions in low-permeability reservoirs. Acta Petrol. Sin. 28 (4), 52–56. https://doi.org/10.1016/S1872-5813(07)60034-6.
Zeng, L.B., Shu, Z., Lyu, W., Zhang, M., Bao, H., Dong, S., Chen, S., Xu, X., 2021. Lamellation fractures in the paleogene continental shale oil reservoirs in the qianjiang depression, jianghan basin, China. Geofluids 2021, 6653299. https://doi.org/10.1155/2021/6653299.
Zeng, L.B., Tang, X., Wang, T., Gong, L., 2012. The influence of fracture cements in tight Paleogene saline lacustrine carbonate reservoirs, western Qaidam Basin, northwest China. AAPG Bull. 96, 2003–2017. https://doi.org/10.1306/04181211090.
Zeng, L.B., Zhou, T.W., Lyu, X.X., 2004. Influence of tectonic compression on the abnormal formation pressure in the Kuga Depression. Geol. Rev. 50 (5), 471–475. https://doi.org/10.16509/j.georeview.2004.05.004.
Zhang, L., Wu, G.H., He, S., She, Z.C., Pan, Y.Y., 2016. Structural diagenesis in carbonate fault damage zone: a case study of the No. 1 fault zone in the Tarim basin. Acta Petrol. Sin. 32, 922–934. CNKI:SUN:YSXB.0.2016-03-023.
Zhang, R.H., Wang, K., Zeng, Q.L., Yu, C.F., Wang, J.P., 2021. Effectiveness and petroleum geological signifcance of tectonic fractures in the ultra-deep zone of the Kuqa foreland thrust belt: a case study of the Cretaceous Bashijiqike Formation in the Keshen gas field. Petrol. Sci. 18, 728–741. https://doi.org/10.1007/s12182-021-00567-w.
Zhang, Y., Chen, Z., Yang, X., Qiao, Y., Teng, Q., Wang, Y., 2020a. Case study: effect of natural fracture on stimulation strategy in keshen tight gas. IOP Conf. Ser. Earth Environ. Sci. 570 (6), 062025 https://doi.org/10.1088/1755-1315/570/6/062025.
Zhang, Y.Z., Feng, J.W., Chang, B.H., Liu, Z.L., Guo, Z.H., 2020b. Control of faultfault-related folds on fracture development in Kuqa depression, Tarim Basin. Oil Gas Geol. 41 (3), 543–557. https://doi.org/10.1007/978-981-16-0761-5_123.
Zhao, W.Z., Xu, C.C., Wang, T.S., Wang, H.J., Wang, Z.C., Bian, C.S., Li, X., 2011. Comparative study of gas accumulations in the permian changxing reefs and triassic feixianguan oolitic reservoirs between longgang and luojiazhai-puguang in the Sichuan Basin. Chin. Sci. Bull. 56, 3310–3320. https://doi.org/10.1007/s11434-011-4668-8.
Zhao, X., Jin, Q., Jin, F., Ma, P., Wang, Q., Wang, J., Ren, C., Xi, Q., 2013. Origin and accumulation of high-maturity oil and gas in deep parts of the Baxian Depression, Bohai Bay Basin, China. Petrol. Sci. 10, 303–313. https://doi.org/10.1007/s12182-013-0279-0.
Zhao, X.Y., Hu, X.Y., Xiao, K.H., Jia, Y.W., 2018. Characteristics and major control factors of natural fractures in carbonate reservoirs of Leikoupo Formation in Pengzhou area, western Sichuan Basin. Oil Gas Geol. 39 (1), 30–39. https://doi.org/10.11743/ogg20180104.
Zhao, Z., Liu, J., Ding, W., Yang, R., Zhao, G., 2021. Analysis of seismic damage zones: a case study of the ordovician formation in the shunbei 5 fault zone, tarim basin, China. J. Mar. Sci. Eng. 9 (6), 630. https://doi.org/10.3390/jmse9060630.
Zhao, R., Zhao, T., Kong, Q., Deng, S., Li, H., 2020. Relationship between fractures, stress, strike-slip fault and reservoir productivity, China Shunbei oil field. Tarim Basin. Carbonate. Evaporites. 35, 84. https://doi.org/10.1007/s13146-020-00612-6.
Zhu, G., Milkov, A.V., Zhang, Z., Sun, C., Zhou, X., Chen, F., Han, J., Zhu, Y., 2019. Formation and preservation of a giant petroleum accumulation in superdeep carbonate reservoirs in the southern Halahatang oil field area, Tarim Basin, China. AAPG Bull. 103, 1703–1743. https://doi.org/10.1306/11211817132.
Zou, C.N., Hou, L., Hu, S., Zhu, R., Liu, S., Yang, Z., Dong, G.Z., Yang, F., Yang, C., 2014. Prospect of ultra-deep petroleum onshore China. Energy Explor. Exploit. 32 (1), 19–40. https://doi.org/10.1260/0144-5987.32.1.19.
Zu, K.W., Zeng, L.B., Gong, L., 2013. Fractures domains in conceptual models of fault-related folds. Chin. J. Geol. 48 (4), 1140–1147. https://doi.org/10.3969/j.issn.0563-5020.2013.04.012.